



Instituto de Neurociencias

Departamento de Bioquímica y Biología Molecular

**Role of the transcriptional coactivator Crtc1 on
hippocampal-dependent associative memory**

**Papel del coactivador transcripcional Crtc1 en la memoria
asociativa dependiente de hipocampo**

Meng Chen

Director: Carlos A.Saura

Doctoral thesis

Bellaterra, Jul. 2014



Instituto de Neurociencias

Departamento de Bioquímica y Biología Molecular

**Role of the transcriptional coactivator Crtc1 on
hippocampal-dependent associative memory**

**Papel del coactivador transcripcional Crtc1 en la memoria
asociativa dependiente de hipocampo**

Memoria de tesis doctoral presentada por *MengChen* para optar al grado de Doctor en neurociencias por la Universitat Autònoma de Barcelona.

Trabajo realizado en la Unidad de Bioquímica y Biología Molecular de la Facultad de Medicina del Departamento de Bioquímica y Biología Molecular de la Universitat Autònoma de Barcelona, y en el Instituto de Neurociencias de la Universitat Autònoma de Barcelona, bajo la dirección del Doctor Carlos Saura Antolín.

El trabajo realizado en esta tesis doctoral ha estado financiado por los proyectos de investigación del Ministerio de Economía y Competitividad (MINECO) “Análisis del transcriptoma en ratones transgénicos de la enfermedad de Alzheimer” (SAF2010-20925) y por el Centro de Investigación Biomédica en Red de Enfermedades Neurodegenerativas (CIBERNED, CB/06/05/0042).

Bellaterra, 18 de Julio de 2014

Doctoranda

Director de tesis

Meng Chen

Carlos A.Saura

Index.....	1
1 List of abbreviations.....	4
2 Abstract.....	8
3 Introduction.....	11
3.1 Alzheimer’s disease.....	12
3.1.1 Alzheimer’s disease etiopathogenesis.....	12
3.1.2 Alzheimer’s disease p neuropathology.....	12
• β -amyloid.....	15
• Tau.....	17
3.1.3 Presenilin.....	18
3.2 Hippocampus-dependent memory.....	23
3.2.1 Associative memory.....	24
3.2.2 Molecular mechanisms mediating memory encoding and storage in the hippocampus.....	27
3.2.3 The transcription factor CREB in learning and memory.....	28
3.2.4 CREB-dependent genes.....	31
o <i>Arc</i>	31
o <i>C-fos</i>	32
o <i>Nr4as</i>	33
3.2.5 Role of CREB signaling in AD.....	34
3.2.6 CREB regulated transcriptional coactivators (CRTC)s.....	35
3.2.6.1 CRTC family members.....	35
3.2.6.2 Function of Crtc in the nervous system.....	39
4 Objectives.....	41
5 Materials and Methods.....	43
5.1 <i>In vivo</i> experimental procedures.....	45
5.1.1 Transgenic mice.....	45
5.1.2 Injection of recombinant AVVs.....	47
5.1.3 Behavior.....	47
5.1.4 Intracardial perfusion and histology.....	48
5.2 Human brain tissue.....	49

5.3	Cell culture.....	49
5.3.1	Primary neuronal culture.....	49
5.3.2	PC12 culture and differentiation.....	51
5.3.3	Transfection and shRNA.....	51
5.3.4	Pharmacological treatments.....	52
5.4	Biochemical methods.....	53
5.4.1	Cell and brain lysis and protein quantification.....	54
5.4.2	Gel electrophoresis and Western blotting.....	54
5.4.3	Dual-luciferase reporter assay	55
5.4.4	Immunoprecipitation.....	55
5.5	Molecular biology methods.....	56
5.5.1	Quantitative RT-PCR.....	56
5.6	Microscope methods.....	57
5.6.1	Immunocytochemistry.....	57
5.6.2	Immunohistochemistry.....	58
5.6.3	Nissl staining.....	59
5.6.4	Image acquisition and processing.....	59
5.7	Statistical analysis.....	59
6	Results.....	60
6.1	Part I : Crtc1 function is critical for contextual fear conditioning.....	61
6.1.1	Activity-dependent Crtc1 nuclear translocation in neurons	61
6.1.2	Contextual learning induces Crtc1 dephosphorylation in the hippocampus.....	64
6.1.3	Contextual learning induces Crtc1 nuclear translocation in the hippocampus.....	67
6.1.4	Contextual learning induces differential expression of Creb/Crtc1-dependent genes.....	70
6.1.5	Age-dependent memory deficits in <i>PS</i> cDKO mice	71
6.1.6	Impairment of Crtc1 nuclear translocation in CA3 hippocampus in <i>PS</i> cDKO mice.....	73
6.1.7	Age-dependent Crtc1-dependent transcriptional deficit in <i>PS</i> cDKO	

mice.....	74
6.1.8 Crtc1 gene transfer reverses Crtc1 transcriptional and associative memory deficits in <i>PS</i> cDKO mice.....	77
6.1.9 Effect of Crtc1 on brain degeneration in <i>PS</i> cDKO mice.....	81
6.1.10 CRTC1 protein changes in human brain at AD pathological stage.....	84
7 Discussion.....	86
8 Hypothesis & Conclusions.....	90
9 Reference List.....	93

Abbreviation

Abbreviations

α CaMKII	Ca ²⁺ /calmodulin-dependent protein kinase II α
AD	Alzheimer's disease
A β	Amyloid- β
AF	Activation function
AMPA	α -Amino-3-hydroxy-5-methyl-4-isoxazolepropionic acid
Aph1	pharynx-defective 1
APLP1	Amyloid-like protein 1
APOE	Apolipoprotein E4 isoform
APP	β -amyloid precursor protein
<i>Arc</i>	<i>Activity-regulated cytoskeleton-associated protein</i>
ATF 1	Acting transcription factor 1
BDNF	Brain-derived neurotrophic factor
BACE	beta-site APP cleaving enzyme 1
bZIP	Basic Leucine Zipper
cAMP	Cyclic adenosine monophosphate
CBP	CREB-binding protein
cKO	Conditional knockout
CR	Conditional responses
CREB	cAMP response element-binding protein
CREM	cAMP response element modulator
CRTC	CREB regulated transcription coactivators
CS	Conditional stimuli
CTF	C-terminal fragment
DBD	DNA-binding domain

DIV	Days in vitro
DNA	Deoxyribonucleic acid
<i>Egr1</i>	<i>early growth response protein 1</i>
ER	Endoplasmic reticulum
ERK	Extracellular signal-regulated kinases
FAD	Familial AD
FTD	Frontotemporal dementia
IEG	Immediate-early gene
LBD	Ligand-binding domain
LTP	Long-term potentiation
MAPK	Mitogen-activated protein kinases
MEF	Myocyte enhancer factor
MSK1	Mitogen and stress-activated kinase 1
Nct	Nicastrin
NFTs	Neurofibrillary tangles
NMDA	N-methyl-D-aspartate receptor
NR	Nuclear receptors
PBS	Phosphate buffered saline
Pen2	Presenilin enhancer 2
PDE4	Phosphodiesterase IV
PKA	Protein kinase
PKC	Protein kinase C
PS	Presenilin
PVH	The paraventricular nucleus
RIN	RNA integrity number

RIPA	Radioimmunoprecipitation assay buffer
SARE	Synaptic activity response element
SD	Splicing domain
SRF	Serum response factor
STM	Short-term memory
TAD	Transactivation domain
TBS	Tris-buffered saline
LTM	long-term memory
US	Unconditional stimulus
VGCC	Voltage-gated calcium channels

Abstract

Abstract

Alzheimer's disease (AD) is an age-dependent neurodegenerative disorder and the main cause of dementia in the elderly. Cognitive decline in AD correlates with synaptic dysfunction and neuron loss, whereas brain functional changes are observed before clinical diagnosis and atrophy of the hippocampus. Besides the classical episodic memory impairment symptoms, dementia patients develop deficits in encoding and retrieval of emotional associative memory and fear conditioning (Granholm and Butters, 1988; Hamann et al., 2002; Sperling et al., 2003; Hofer et al., 2008; van der Meulen et al., 2012). Persons with risk for developing AD show impaired associative emotional encoding and conditioned responses (Sperling et al., 2003; Hofer et al., 2008; Parra et al., 2013). Despite the evidence for emotional learning and memory deficits in dementia, the molecular mechanisms involved are largely unknown.

The cAMP-response element binding protein (CREB) signaling pathway regulates gene expression programs mediating synaptic plasticity and memory. Recent evidences suggest that deregulation of cAMP/Ca²⁺-mediated CREB signaling negatively affect hippocampal synaptic plasticity, memory and synapse loss in AD models (Vitolo et al., 2002; Smith et al., 2009; España et al., 2010). These results suggest that disruption of CREB signaling may contribute to memory deficits in AD (Saura and Valero, 2011). However, the specific role of CREB and its transcriptional coactivator Crtc1 on gene transcription during associative memory in normal and neurodegenerative conditions are unknown.

In this doctoral thesis, we investigated the specific role of the CREB transcriptional coactivator Crtc1 in associative memory in physiological and pathological conditions. In cultured primary neurons, Crtc1 is rapidly (min) dephosphorylated and translocated to the nucleus upon synaptic stimulation indicating that Crtc1 is activated by dephosphorylation. By using fear conditioning, we found that context conditioning induces rapid translocation (15 min) of Crtc1 from the cytosol to the nucleus of neurons in the CA1 and CA3 regions of the adult mouse hippocampus. Crtc1 nuclear translocation is associated with Crtc1 dephosphorylation at Ser151, a residue critical for transcriptional

activation, whereas Creb phosphorylation (Ser133) is induced independently of a paired unconditioned stimulus. Interestingly, Crtc1 dephosphorylation is induced specifically in the hippocampus by context conditioning but not by context encoding or shock stimuli. Contextual conditioning but not context encoding or shock up regulates gene expression levels including *c-fos* and the Nr4a family members *Nr4a 1* and *2* genes in a Crtc1-dependent manner. Notably, reduced Crtc1 nuclear translocation and Crtc1-dependent transcription is associated with long-term contextual memory impairments in a mouse model of neurodegeneration lacking the presenilin genes (*PS cDKO*). In addition, adeno-associated viral-Crtc1 gene transfer in the hippocampus reverses hippocampal Crtc1-dependent transcription changes and associative memory deficits despite unchanged cortical degeneration in *PS cDKO* mice. Finally, post mortem analysis shows that CRT1 levels are reduced in human hippocampus at intermediate Braak III/IV pathological stages.

These findings reveal a critical role of Crtc1 nuclear translocation and transcriptional function in contextual memory encoding in physiological and neurodegenerative conditions.

Introduction

Introduction

3.1 Alzheimer's disease

3.1.1 Alzheimer's disease etiopathogenesis

Alzheimer's disease (AD) is the most common form of dementia among the elderly and characterized clinically by progressive deterioration of memory and other cognitive functions. In 2010, 35.6 million people were estimated to be living with dementia. The total number of people with dementia is projected to almost double every 20 years, to 65.7 million in 2030 and 115.4 million in 2050. The total number of new cases of dementia each year worldwide is nearly 7.7 million, implying one new case every four seconds (WHO, 2012).

The principal risk factor for AD is aging. According to different estimates, the prevalence doubles every five years after the age of 65 (WHO, 2012). More than 95% of AD cases are sporadic, whereas less than 5% of cases are considered as early-onset AD because start before the age of 65. The majority of early-onset AD cases are linked to mutations in genes encoding presenilin 1 (*PSEN 1*; *PS1*), presenilin 2 (*PSEN 2*; *PS2*) and β -amyloid precursor protein (*APP*). Although the underlying mechanism(s) leading to the development of sporadic AD are still not known, several potential risk genes have been identified (Ballard et al., 2011; Table 1). The main genetic risk factor of late-onset AD is the apolipoprotein E 4 isoform (*APOE4*) (Corder, et al., 1993). *SORL1* has also been identified as an important genetic cause of late-onset AD (Rogaeva et al., 2007).

3.1.2 Alzheimer's disease neuropathology

The neuropathological hallmarks of AD are progressive and selective loss of neurons and synapses, deposition of extracellular amyloid- β ($A\beta$) peptides in senile

plaques and formation of intracellular neurofibrillary tangles (NFTs). Since synaptic and neuronal dysfunction are evident at very early stages of the disease, loss of synapses

Role in Alzheimer's disease	Effect on risk of Alzheimer's disease
Familial genes	
APP APP is a membrane protein cleaved by secretases. Cleavage of APP by secretases leads to both non-amyloidogenic processing and production of A β . Familial APP mutations result in preferential processing of APP through the amyloidogenic pathway ²³	NA
PSEN1 PSEN1 is a component of α secretase, which is involved in APP processing to A β . Familial PSEN1 mutations can alter the production of A β_{1-40} , which forms plaques more readily than A β_{1-42} ²⁴	NA
PSEN2 Processes APP into A β as part of the α -secretase complex. Familial mutations can alter the production of A β_{1-42} , which forms plaques more readily than A β_{1-40} ²⁵	NA
Sort1 Sort1 interacts with APP, affects APP trafficking, and overexpression of the protein results in reduced A β production. Binding of Sort1 to APP results in reduced A β production. SORL1 is a γ -secretase substrate. Sort1 concentrations are reduced in patients with Alzheimer's disease ²⁶	NA
Risk genes	
APOE APOE is transported with cholesterol, APOE isoforms have differing transport efficiencies. APOE binds A β in an isoform-specific manner. APOE is involved in A β clearance through interaction with LRP. APOE4 alleles are associated with increased amyloid burden and cholinergic dysfunction	3-10 times increased ²⁷
GSK3β GSK3 β phosphorylates tau, leading to tangle formation. APP cleavage products can activate GSK3 β , leading to increased tau phosphorylation. GSK3 β phosphorylates tau more effectively if tau has already been phosphorylated by other kinases, such as cdk5. GSK3 β activity can also be promoted by PSEN complexes	1.7 times increased. ^{28,29} No Alzgene meta-analysis
DYRK1A DYRK1A is located on chromosome 21. DYRK1A is involved in tau phosphorylation; its activity is upregulated by A β , therefore DYRK1A is a link between amyloid and tau pathologies. DYRK1A phosphorylates tau to prime the molecule for further phosphorylation by GSK3 β . DYRK1A also phosphorylates septin 4, another tangle protein. DYRK1A is involved in APP phosphorylation, which leads to increased amyloidogenic processing through increased BACE interaction	T allele is less frequent in people with Alzheimer's disease. No Alzgene meta-analysis ³⁰
Tau Tau is hyperphosphorylated in NFTs. Tau exists as six splice isoforms depending upon inclusion of N-terminal exons 2 and 3, and the exon 10 microtubule binding domain. Tau mutations can affect splicing and microtubule binding efficacy. The tau haplotype is associated with Alzheimer's disease, and affects expression levels of tau splice isoforms	H1C haplotype more frequent in Alzheimer's disease. No Alzgene meta-analysis of the haplotype ^{31,32}
TOMM40 TOMM40 is a translocase of outer mitochondrial membrane 40 homolog on the same chromosome as APOE. TOMM40 interacts with APP and is associated with the age of onset in late-onset Alzheimer's disease ³³	Alzgene odds ratio of 0.66 for rs8106922
CLU Clusterin is a chaperone involved in A β formation and is associated with severity and progression of Alzheimer's disease ³⁴	Alzgene odds ratio of 0.87 for rs1113600
PIGALM Phosphatidylinositol binding clathrin assembly protein, present in endosomes which are enlarged in early Alzheimer's disease ³⁵	Alzgene odds ratio of 0.87 for rs541458

A full meta-analysis of risk genes can be found on the Alzgene website (<http://www.alzgene.org/>). NA=not applicable. A β =amyloid β . APP=amyloid precursor protein. APOE=apolipoprotein E. NFT=neurofibrillary tangle.

Table 1: Genes linked to Alzheimer's disease (Ballard C et al., 2011)

could be associated with early synaptic and memory dysfunction (Scheff and Price, 2003). Current evidence strongly supports the notion that the initiating event in AD is related to abnormal processing of A β ultimately leading to its accumulation in A β plaques (Jack et al., 2010). This process might occur in presymptomatic stages while the individuals are quite cognitively normal, preceding symptomatic stages characterized by gross neuronal dysfunction, neurofibrillary tangles accumulation and neurodegeneration (Jack et al., 2010). Some neurodegenerative dementias, such as frontotemporal dementia (FTD), occur in the absence of A β plaques suggesting that A β accumulation is not a central feature of all dementias.

The neuropathological progression of AD occurs in different stages named Braak stages I to VI classified according to neurofibrillary tangles and neuropil threads. Braak stage 0 is used to indicate the absence of any neurofibrillary changes. In Braak stage I and II (transentorhinal stages), slight pathological changes present in the transentorhinal cortex, but there is no cognitive decline. In Braak stage III and IV (limbic stages), the neurofibrillary changes extend to the transentorhinal cortex, hippocampus and

limbic area. Patients suffer from a mild cognitive impairment. In Braak stage V and VI (isocortical stages), most of the isocortical association areas are affected by neurofibrillary changes, and patients are diagnosed with dementia (Braak and Braake, 1991; Gauthier, et al., 2006; Braak, et al., 2006; Thal, et al., 2002; Figure 1).

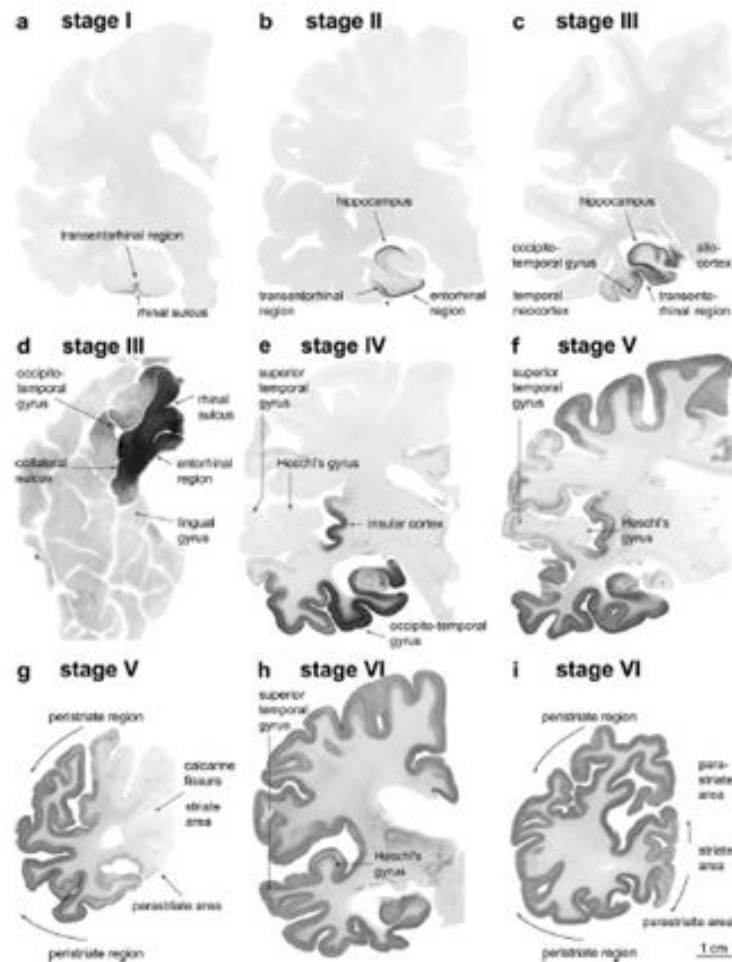


Figure 1. AD neuropathological stages in human brain. Immunohistological characterization of cortical neurofibrillary stages I–VI in 100 μm polyethylene glycol-embedded hemisphere sections immunostained for hyperphosphorylated tau (AT8, Innogenetics) (Braak H et al., 2006)

3.1.2.1. β -amyloid

Neuritic plaques are formed by extracellular deposits of aggregated $A\beta$ peptides (Glennner and Wong, 1984). $A\beta$ are 38 to 43 amino acid peptides formed as products of the proteolytic processing of the APP. Three protease activities called α -, β -, and γ -secretase are involved in specific processing of APP (Haass, 2004), which occurs through two main pathways: the amyloidogenic and the non-amyloidogenic pathways. In the amyloidogenic pathway APP undergoes ectodomain shedding by β -secretase (BACE) and produce β -CTF (or C99) fragments which is then cleaved by γ -secretase to generate $A\beta$ (Haass et al., 2012). In the non-amyloidogenic pathway, APP is cleaved by α -secretase to produce α -CTF (or C83) that is cleaved by γ -secretase to release a small peptide called p3 (Haass et al., 2012, Figure 2).

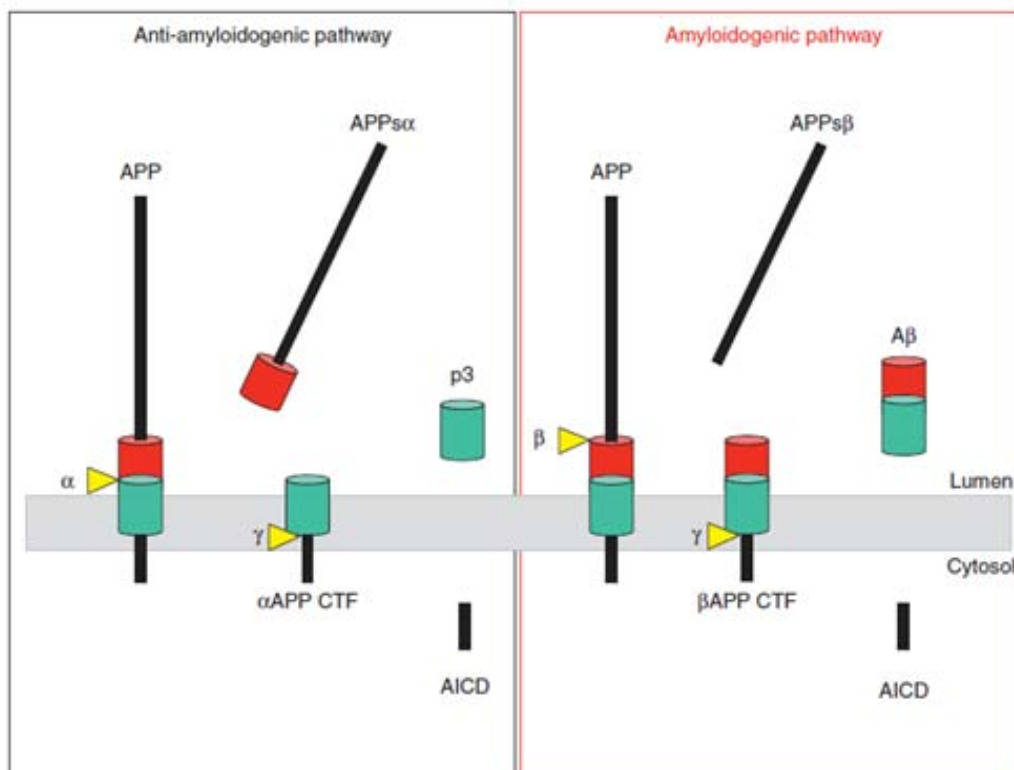


Figure 2. Proteolytic processing of APP within the anti-amyloidogenic (left) and amyloidogenic (right) pathways (Haass C, 2012).

Under physiological conditions, approximately 90% of secreted $A\beta$ is $A\beta_{40}$, while 10% is $A\beta_{42}$. The $A\beta_{42}$ is more prone to aggregate than $A\beta_{40}$ and the ratio of these two isoforms is affected by enzymatic cleavages of α - or β - and γ -secretases (Hardy, 2006). $A\beta$ self-aggregates into different coexisting forms. One form consists of oligomers formed by 2 to 6 monomers. $A\beta$ can also form insoluble fibrils. It is currently thought that the small soluble oligomers are more toxic than the insoluble fibrils. The toxic effect of oligomers, not the total $A\beta$ burden, causes synaptic changes and neuronal dysfunction and death (Lue, 1999; Ballard, et al., 2011; Figure 3).

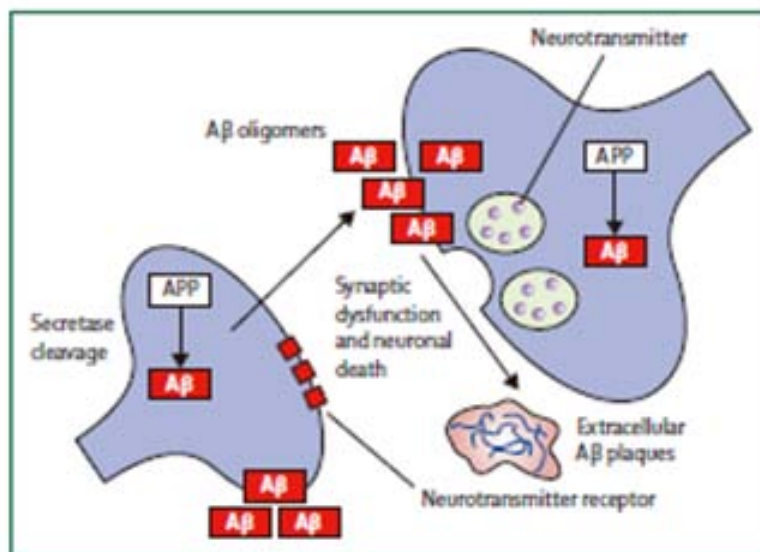


Figure 3: Amyloid cascade hypothesis

APP is processed into $A\beta$, which accumulates inside neuronal cells and extracellularly, where it aggregates into plaques. In the amyloid cascade hypothesis, these $A\beta$ deposits are toxic and cause synaptic dysfunction and neuronal cell death. (Ballard C., et al., 2011)

3.1.2.2. Tau

NFTs are present in the brain of AD and other dementing disorders such as FTD (Ballatore, 2007; Lee, 2001). The major component of tangles is the paired helical filaments formed by the microtubule-associated protein tau. In normal conditions, tau is soluble protein that assembles and stabilizes the microtubules allowing axonal vesicle transport. In pathological conditions, tau is abnormally hyperphosphorylated and aggregated, so insoluble forms of tau reduce their affinity for microtubules (Figure 4). The aggregates of tau are cytotoxic and impair cognition (Khlistunova, 2006; Santacruz, 2005; Oddo, 2006). The correlations of NFTs density and cognitive decline in AD suggest that tau plays an important role in pathology. However, *tau* mutations have not been detected in AD.

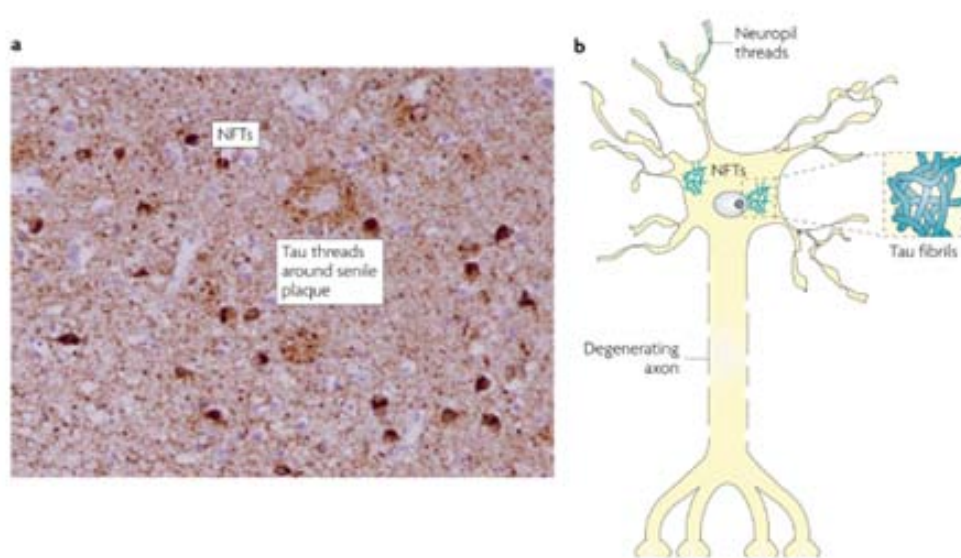


Figure 4. Tau pathology in AD and related tauopathies

At autopsy, the brains of patients with Alzheimer's disease or related tauopathies show abundant neurofibrillary tangles (NFTs) and neurofilament threads that are formed by pathological phosphorylated tau. These tau deposits can be visualized by treating brain slices with certain silver stains or by immunostaining with antibodies that recognize tau (A). Schematic representation of NFTs and neurofilament threads within a neuron is shown in B, with an example of tau fibrils that resemble those found in NFTs depicted in the inset. (Brunden KR, 2009)

3.1.3 Presenilins

Presenilins (PS) are membrane proteins containing 9 transmembrane domains (Laudon, et al., 2005). They are present in the endoplasmic reticulum (ER) and other compartments in neurons but also broadly expressed in different tissues (Walter, et al., 1996). Under physiological condition, PS undergoes endoproteolysis to generate N-terminal and C-terminal fragment (Thinakaran, et al., 1996). The mammalian PS genes, presenilin 1 (PSEN1) and presenilin 2 (PSEN2), share a high degree of homology at the protein sequence (67%) and functional redundancy (Lleó and Saura, 2011).

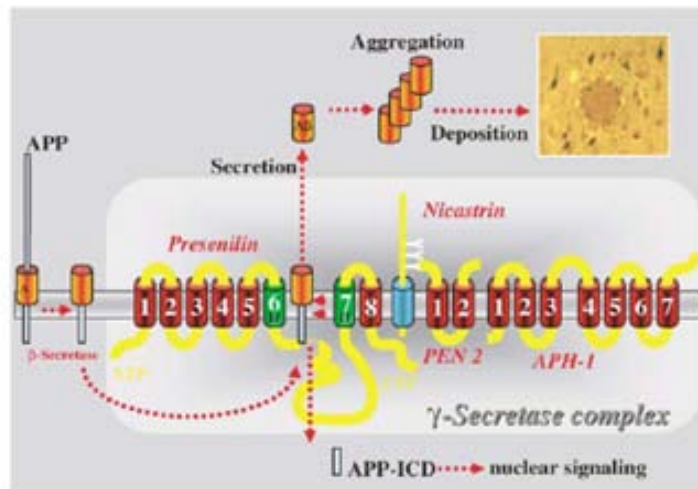


Figure 5 Generation of Ab from APP via proteolytic processing by β - and γ -secretase.

Ab aggregates and finally precipitates in amyloid plaques. This event initiates the amyloid cascade resulting in additional intracellular aggregations of the tau protein, which then form tangles. (Haass C, 2004)

PS together with anterior pharynx-defective 1 (Aph1), presenilin enhancer 2 (Pen2) and nicastrin (Nct) are integral components of the multiprotein protease complex γ -secretase, which is responsible for the intermembranous cleavage of type I transmembrane proteins, including among others APP, APLP-1, Notch, or CD44

(Fortini, 2002, Figure 5). The general requirements to be cleaved efficiently by γ -secretase are a type I transmembrane helix and a small ectodomain, permissive transmembrane and cytoplasmic domains (Lleó and Saura, 2011). Presenilins are essential for γ -secretase activity since their inactivation impairs A β generation and accumulation *in vitro* and *in vivo* (De Strooper, 1998; Yu, Saura, et al., 2001; Saura et al., 2005).

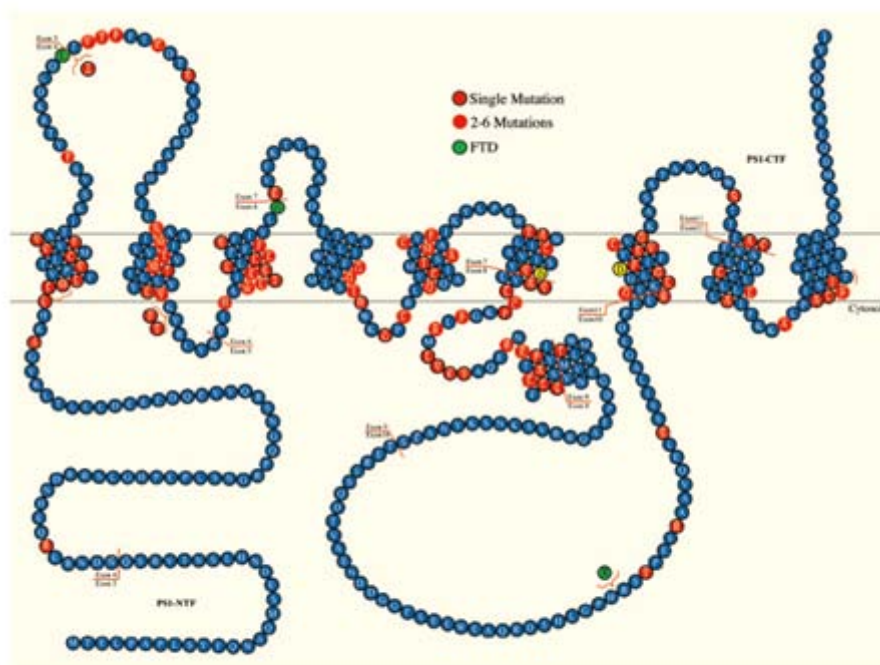


Figure 6 Large numbers of pathogenic PS1 mutations are diffusely distributed throughout the coding sequence (Shen J and Kelleher RJ 3rd, 2006).

Presenilins were first identified in screens for mutations causing early onset forms of familial AD by Peter St George-Hyslop in 1995. *Presenilin-1 (PS1)* is located on human chromosome 14 and *Presenilin-2 (PS2)* is located on chromosome 1. Dominantly inherited mutations in *PS1* and *PS2* contribute to approximately 90% of familial AD (FAD), although most of them have been identified in *PS1*. More than 150 mutations in the PS1 have been identified in different families with FAD (Hutton M. and Hardy, 1997, Figure 6). PS mutations enhance selectively production of the amyloidogenic A β 42

peptides, often at the expense of the less amyloidogenic A β 40 (Moehlmann, 2002). PS mutations can cause neurodegenerative dementia in the absence of A β accumulation suggesting that PS mutations may cause neurodegeneration through other pathogenic mechanisms (Shen, and Kelleher, 2007). For instance, PS1 mutations (L113P, G183V AND insR352) have been identified in FTD cases characterized by phosphorylated tau accumulation in the absence of Ab. In conclusion, the pathogenic mechanisms by which presenilin mutations cause memory loss and neurodegeneration remain still largely unclear.

Increasing evidence shows that PSs also carry out γ -secretase-independent activities involved in Wnt/ β -catenin signaling pathway, cell adhesion, calcium release, lysosomal proteolysis and apoptosis (Tu, et al., 2006; Lee, et al., 2010). Thus, presenilins play essential roles during development. Mice lacking PS1 or both PS during embryogenesis display perinatal lethality and skeletal and neural developmental defects (Shen, et al., 1997; Donoviel, et al., 1999; Handler, et al., 2000). Presenilins are implicated in the processing of Notch receptor, an important developmental protein, and play a major role in the maintenance of the neural progenitor population through the Notch signaling pathway (Kim and Shen, 2008).

In the adult brain, presenilin is expressed highly in excitatory neurons of the cerebral cortex, and is required for hippocampal-dependent synaptic plasticity and memory (Ho and Shen, 2011; Table 2). In contrast to the embryonic lethality of PS null mice, brain-specific *PS1* conditional knockout (cKO), in which expression of PS1 is selectively eliminated in excitatory neurons of the forebrain beginning at postnatal day ~18 (Yu, 2001) exhibit normal hippocampal synaptic transmission and plasticity subtle spatial memory deficits (Yu, 2001).

Presenilin knockouts ^a	Synaptic deficits ^b	Cognitive deficits ^c	Neuronal loss ^d	Refs.
FB-PS1 cKO (3-6 months)	--I/O --PPF	--LTP (TBS) --LTP, L-LTP (HFS) --LTD (ppLFS)	Mild deficits in spatial learning and memory	--Cortical volume --Cortical neuronal number Yu et al., 2001
FB-PS cDKO (2 months)	--I/O]PPF]Synaptic facilitation]Pr (unitary responses)]NMDAR function]LTP (TBS, pairing) --LTD (ppLFS)	Impaired spatial and associative memory	--Cortical volume --Cortical neuronal number]Apoptotic cells Saura et al., 2004 Whee-Samuelson et al., 2010 Zhang et al., 2010
FB-PS cDKO (8 months)]PPF]Maximal fiber volley]I/O]NMDAR function]LTP (TBS, pairing) --LTD (ppLFS)	Severely impaired spatial associative memory]Cortical volume]Cortical neuronal number Saura et al., 2004 Feng et al., 2004 Whee-Samuelson et al., 2010
CA3-PS cDKO (2 months)]PPF]Synaptic facilitation]Pr (MK-801)	--NMDAR function]LTP	N/A	N/A Zhang et al., 2009
CA1-PS cDKO (2 months)	--PPF --Synaptic facilitation	--NMDAR function --LTP	N/A	N/A Zhang et al., 2009

Table 2. Role of presenilins in synaptic plasticity, learning and memory, and neuronal survival in the adult cerebral cortex

^aCA1-PS cDKO, inactivation by conditional double knockout of presenilins in CA1 neurons; CA3-PS cDKO, inactivation by conditional double knockout of presenilins in CA3 neurons; FB-PS1 cKO, forebrain PS1 conditional knockout; FB-PS cDKO, forebrain PS conditional double knockout.

^bI/O, input-output; LTD (ppLFS), long-term depression (paired-pulse low-frequency stimulation); L-LTP (HFS), late phase of long-term potentiation (high-frequency stimulation); LTP (TBS), long-term potentiation (theta burst stimulation); NMDAR, N-methyl-D-aspartic acid receptor; PPF, pair-pulse facilitation; Pr, release probability.

^cN/A, not available. (Adapted from Ho A and Shen J, 2011)

Presenilin conditional double knockout (*PS* cDKO) mice lacking both PS1 and PS2 in the postnatal forebrain display age-dependent synaptic plasticity and memory deficits. Loss of PS function results in selective impairment in long-term potentiation (LTP) which is a measure of experience-dependent synaptic strengthening. LTP deficits in *PS* cDKO mice are associated with reduced NMDAR-mediated synaptic responses (Saura, et al., 2004). PS also participate in the release of neurotransmitter during synaptic transmission. Specific knockout presenilins in presynaptic (CA3) or postsynaptic (CA1) neurons of the hippocampal Schaffer collateral pathway (Figure 7) shown that presynaptic, but not postsynaptic inactivation of presenilins, leads to inhibition of theta burst induced LTP. Decreased level of glutamate release contributes to LTP deficits.

Moreover, depletion of the endoplasmic reticulum (ER) Ca^{2+} storage and blockade of intracellular Ca^{2+} release mimicked the effect of presynaptic presenilin in active. LTP deficits and inhibition of glutamate release by regulating Ca^{2+} release from intracellular stores (Zhang, et al., 2009; Ho and Shen, 2011). In addition, loss of neuronal PS leads to a selective reduction in synaptic NMDA receptor levels and responses, as well as decreased α CaMKII, CBP and CREB/CBP target genes (Saura et al., 2004). Finally, *PS* cDKO mice develop subsequently age-dependent synaptic, dendritic and neuronal degeneration (Figure 8) with accompanying astrogliosis and hyperphosphorylation of tau, demonstrating an essential role for PS in neuronal survival (Saura, et al., 2004).

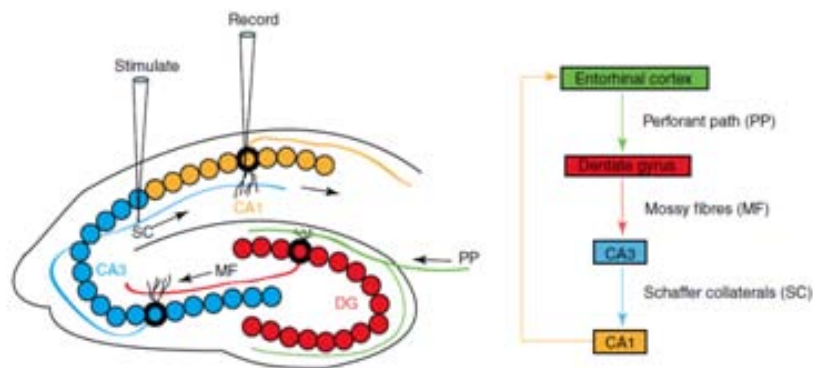


Figure 7. The hippocampal network

The hippocampus forms a unidirectional neural network with input arising from the entorhinal cortex that forms synaptic connections with the dentate gyrus (DG) via the perforant path (PP). Axons from DG project to CA3 pyramidal neurons via the mossy fibers (MF) pathway. Axons from CA3 project to CA1 pyramidal neurons via the Schaffer collateral (SC) pathway. These CA1 neurons in turn send the main output back to the entorhinal cortex. CA3 and CA1 neurons can also receive input directly from the perforant path (Ho A. and Shen J., 2011)

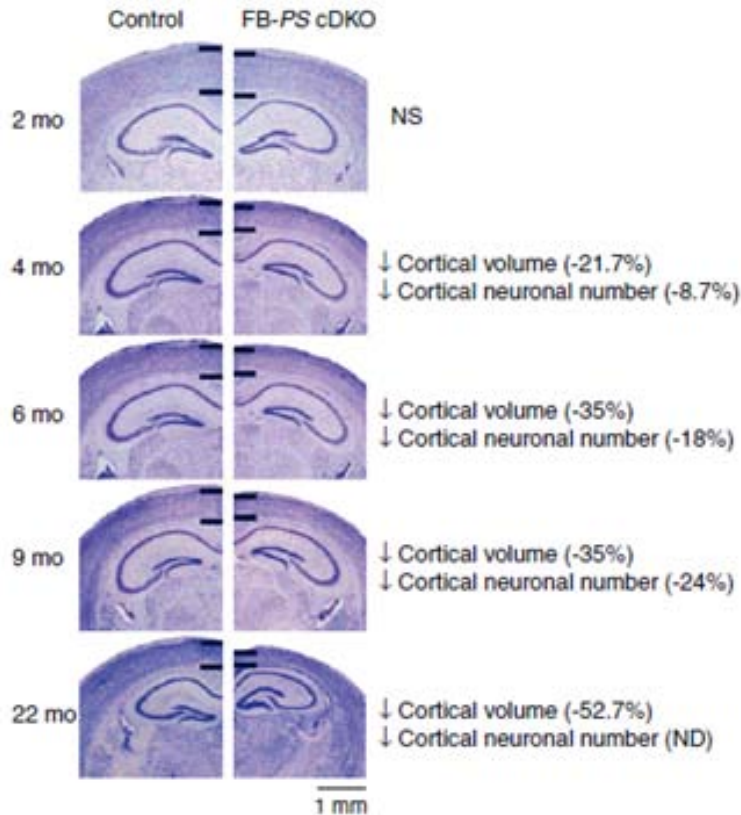


Figure 8. Cortical degeneration in PS cDKO mice.

Black horizontal bars delineate neocortical layers. At 2 months, no detectable difference is found in size or shape of the PS cDKO brain relative to control. However, subsequent ages reveal a gradual decrease in cortical thickness in PSEN cDKO mice.

Scale bar: 1 mm (Wines-Samuelson M et al., 2010; Ho A and Shen J, 2011).

3.2 Hippocampus-dependent memory

Memory is the process in which information is encoded, stored, and retrieved. Learning is considered as a way to acquisition and encoding the information to memory. Short-term memory (STM) is reflected by a rapid decay of the newly acquired neural response. STM is temporary and subject to disruption, while long-term memory (LTM), once consolidated, is persistent and stable. Consolidation of STM into LTM at the

molecular level presumably involves synaptic changes, such as LTP and LDP.

Hippocampus is critical to the consolidation of information from short-term to long-term memory. Studies in higher primates and humans have demonstrated that hippocampus is required for spatial learning, declarative memory (Squire and Zola-Morgan, 1991) or episodic memory (Tulving et al., 1994). In addition, the hippocampus has been thought to be involved in several memory processes, such as encoding, consolidation, and retrieval. Lesion studies in animals support a requirement of the hippocampus in the process of long-term memory formation (Anagnostaras, et al., 1999), and the damage limited in hippocampus is sufficient to cause memory deficit (Zola-Morgan et al., 1992). The hippocampal structure is functionally heterogeneous as different portions of the longitudinal axis sharing different functional roles, due to differences in connectivity (Moser and Moser, 1998). Indeed, the dorsal (septal) hippocampus seems to be highly involved in spatial learning (Moser and Moser, 1998), which is consistent with the major visual-spatial inputs received from the temporal and parietal cortices, whereas the ventral (temporal) hippocampus has a strong connectivity with the hypothalamus and the amygdala, which potentially accounts for the hippocampal participation on emotion (Kjelstrup et al., 2002).

3.2.1 Associative memory

Associative memories elicited by learning new information of people, places or locations and are essential for recollecting the past interpreting the present and anticipating the future, etc.

Contextual fear conditioning is a hippocampus-dependent task that involves a learned process including a specific training context and an aversive foot-shock (Maren, 2008). In fear conditioning, conditional stimuli (CSs) such as tones, lights, or places

(contexts) are arranged to indicate aversive outcomes such as footshock (an unconditional stimulus, US). After conditioning, CSs lead to learned fear responses (conditional responses or CRs) such as conditioned freezing (Maren, 2008). Thus, during a typical context fear-conditioning training, animals first encode a representation of the context (when the animal explores the context before a footshock) and then associate that representation with the US. These two learning stages are referred to as context encoding and context conditioning, respectively (Maren et al., 2013). Context encoding is necessary for context conditioning. Animals do not show context conditioning if they are shocked immediately when placed into chamber (Maren et al., 2013).

The hippocampus and amygdala are two brain areas that play a critical role in conditioned freezing behavior. Whereas the amygdala was participated in learning about both contextual and discrete (e.g. cues) stimuli (Phillips & LeDoux, 1992), the hippocampus plays a selective role in fear in response to contextual stimuli (Phillips & LeDoux, 1992; Maren, 2008). These tasks are often considered as a way to index 'hippocampal-dependent' contextual conditioning and 'hippocampal-independent' cue conditioning in the same animal (Maren, 2008). Despite this, hippocampus-amygdala interactions are involved in the contextual fear memories (Figure 9).

Several subregions of hippocampus are involved in associative memory. CA1 and CA3 hippocampus are involved in the acquisition and encoding contextual fear memory. CA3 is involved in the rapid formation of the representation of the context and a configural representation of numerous spatial cues can be initially formed and stored for a short-time period during acquisition. The DG functions as a pattern separator that can input patterns needed to be further differentiated from each other before they reach CA3 (Treves and Rolls, 1994). Therefore, the DG-CA3 network may play a critical role in the initial phase of the acquisition of context-specific fear memory. The CA1 hippocampal subregion has been considered as an output structure from the hippocampal network to the neocortex.

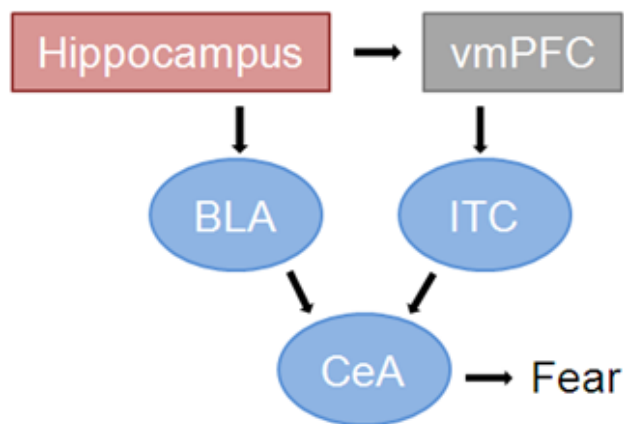


Figure 9. A simplified anatomical diagram of connections among brain structures involved in fear conditioning.

The hippocampal region projects to both vmPFC and amygdala. The amygdala has different nuclei; each has different connectivity patterns to afferent structures, and plays different connectivity patterns to afferent structures, and play different function in fear conditioning. vmPFC, ventromedial prefrontal cortex; ITC, intercalated cells of the amygdala; BLA, basolateral nucleus of the amygdala; CeA, central nucleus of the amygdala.

3.2.1 Associative memory in dementia

Persons with risk for developing Alzheimer's disease (AD) show impaired associative emotional encoding and reduced conditioned responses associated with disrupted hippocampal and amygdala functional connectivity (Sperling et al., 2003; Hofer et al., 2008; Parra et al., 2013). Dementia patients develop deficits in encoding and retrieval of emotional associative memory and fear conditioning (Granholm and Butters, 1988; Hamann et al., 2002; Sperling et al., 2003; Hofer et al., 2008; van der

Meulen et al., 2012). Despite the evidence for emotional learning and memory deficits in dementia, the molecular mechanisms involved are largely unknown.

3.2.2 Molecular mechanisms mediating memory encoding and storage in the hippocampus

Santiago Ramón y Cajal originally hypothesized that the potential of the brain to adapt to the environment could involve the reinforcement of pre-existing neural connections by means of structural changes that would improve the efficiency of neuronal circuits (Ramón y Cajal, 1894). Cajal's modern view postulates that the strength of synaptic connections or plastic changes that persist for days or much longer as a result of training and learning induces memory formation. Activity-dependent reinforcement and refinement of synaptic connections occurs during development and in the adult brain. These synaptic plastic changes are mediated by long-lasting structural changes at synapses that require activation of gene expression programs (Saura and Valero, 2011).

Long-lasting synaptic plasticity and memory require activity-dependent gene transcription and synthesis of new proteins (Kandel, 2001). Gene transcription mediates long-lasting changes of synaptic efficacy essential for synaptic plasticity and memory (Guzowski et al., 2001; Cohen and Greenberg, 2008). To date, a large number of transcription factors and molecules have been identified to control many biological processes through regulation of gene expression (Dymlacht, 1997).

During fear conditioning, the presentation of CS and US triggers activation of protein kinase/phosphatase pathways which can cause changes on transcription factors activity in hippocampal and amygdale neurons. These molecular changes are significantly higher when the CS and US are presented in a paired way than when the CS is performed alone. The same rule applies to downstream target: the CREB and the immediate-early genes (IEGs), *activity-regulated cytoskeleton-associated protein (Arc)*, *c-fos* and *early growth response protein 1 (Egr-1)*; also the whole family of CRE-regulated genes. In

addition, key regulators of the calcium/calmodulin kinase II (CaMKII) pathway are not activated by context alone but are strongly upregulated by context and shock. These CS/US-specific signaling patterns provide convincing evidence for differential processing of the CS in the presence or absence of US (Tronson et al., 2012). In addition, the cAMP and ERK/MAP kinase (MAPK) signaling is also involved in hippocampus-dependent memory through CREB-mediated transcription. The study demonstrates that cAMP-dependent protein kinase (PKA), MAPK, mitogen and stress-activated kinase 1 (MSK1) and CREB has been activated in hippocampus CA1 pyramidal neurons following contextual fear conditioning through Ca^{2+} -stimulated adenyl cyclase activity (Sindreu et al., 2007).

3.2.3 The transcription factor CREB in learning and memory

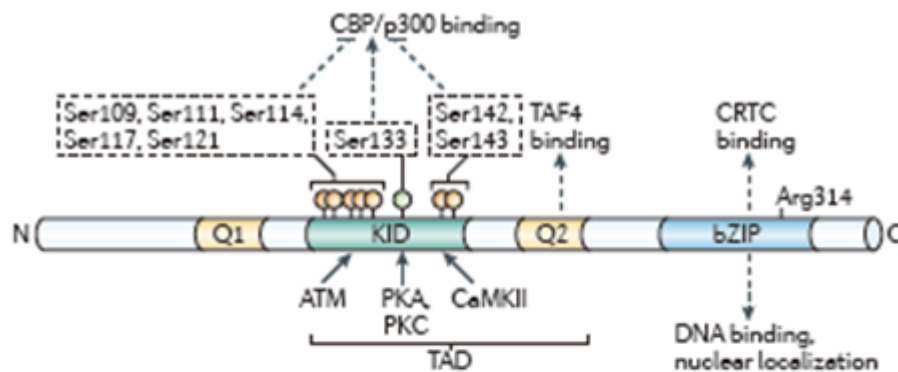


Figure 10. Modular organization of CREB

CREB contains two Glu-rich domains (Q1 and Q2), a central kinase-inducible domain (KID) and a carboxy-terminal basic Leu zipper (bZIP) domain. The KID domain and the Q2 domain make up the amino-terminal transactivation domain (TAD). Phosphorylation of the KID domain at Ser133 promotes an interaction with CREB-binding protein (CBP) and its paralogue p300. Two clusters of phosphorylation sites flanking Ser133 inhibit CBP/p300 binding. The bZIP domain promotes CREB DNA binding and dimerization; it also mediates CREB binding to cAMP-regulated transcriptional co-activators (CRTCs). Arg314 in the bZIP domain is critical for the CREB–CRTC interaction. (Altarejos J.Y. and Montminy M. 2011).

The transcription factor CREB is a 43 kDa protein and binds to the highly conserved CRE palindromic sequence 5'-TGACGTCA-3' or half-site sequence 5'-TGACG-3' or 5'-CGTCA-3' (Montminy, et al. 1986; Comb, et al. 1999). CREB belongs to the bZIP superfamily of transcription factors that includes CREB, the cAMP response element modulator (CREM) and the activating transcription factor 1 (ATF-1) (Lonze and Ginty, 2002). CREB and its family members are structurally characterized by an amino-terminal transactivation domain (TAD) and a carboxy-terminal basic Leu zipper (bZIP) DNA-binding and dimerization domain (Altarejos and Montminy, 2011; Figure 10).

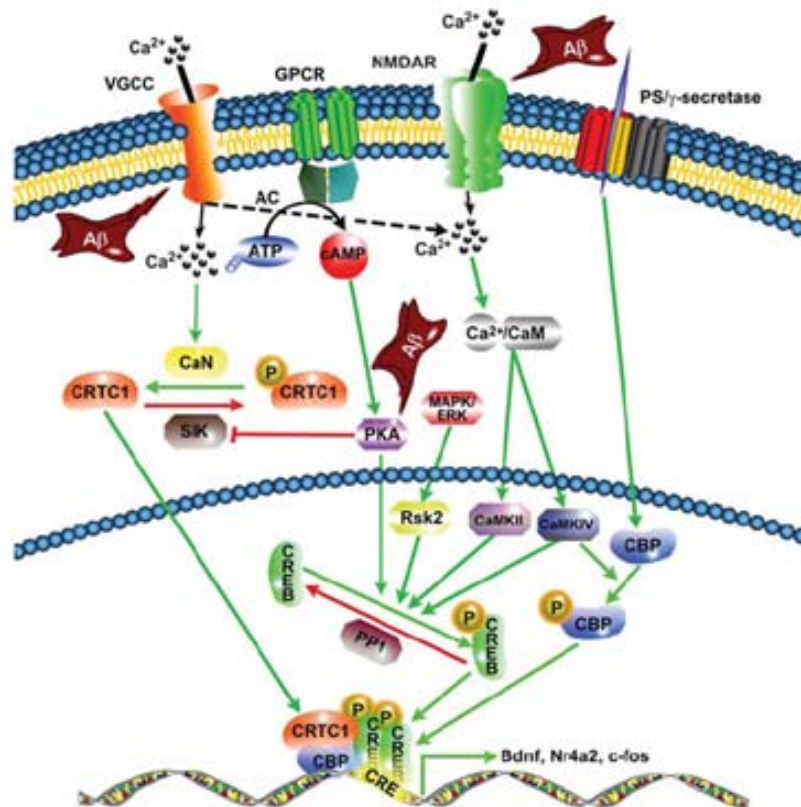


Figure 11. Signaling pathways regulating CREB-dependent transcription in neurons

CREB-dependent transcription depends on multiple cellular mechanisms that act in concert with CREB phosphorylation on Ser133, including additional phosphorylation events and binding to the transcriptional machinery through coactivators such as CRTCs or CBP. (Saura and Valero, 2011)

CREB transcriptional activation depends on calcium- and cAMP-dependent phosphorylation of CREB at Ser133 (Sheng et al., 1991; Mayr and Montminy, 2001). CREB contains consensus sites for several kinases that regulate CREB transcriptional activity (Gonzalez and Montminy, 1989). Ca^{2+} /calmodulin (CaM)-dependent protein kinases CaMKII and CaMKIV, ras-mitogen-activated protein kinase (MAPK/ERK), MAPK-activated kinase RSK and cAMP-dependent protein kinase A (PKA) are kinases that participate to mediate CREB phosphorylation at Ser133 (Deisseroth and Tsien, 2002; Saura, 2011; Figure 11). Calcium influx through L-type voltage-gated calcium channels (VGCCs) or glutamate ligand-gated ion channels (NMDA and AMPA) is crucial for CREB phosphorylation and nuclear translocation.

However, phosphorylation at Ser 133 is important to stimulate CREB activity but it is not sufficient for gene transcription. The timing and duration of CREB phosphorylation is critical for CREB-mediated transcription. The rapid phosphorylation of CREB is associated to CaMKIV pathway and induced by neuronal

activation including depolarization, synaptic stimulation and behavioral training (Bitto, et al., 1996). While both CaMKIV and Ras/MAPK mediate long-lasting phosphorylation which is related to gene expression (Wu, et al., 2001). However, selective gene transcription by CREB depends on additional events including other phosphorylation sites and recruitment of specific coactivators (Cohen and Greenberg, 2008; Saura, 2011; Figure 12). For instance, phosphorylation of CREB on Ser142 and Ser143 participates in Ca^{2+} -dependent gene transcription (Kornhauser, et al., 2002).

CREB is essential for synaptic plasticity and long-term memory (Bourtchuladze et al., 1994; Won and Silva, 2008). CREB is widely expressed in the brain and especially areas associated with learning and memory, including the hippocampus and cortex. In *Drosophila*, expression of a dominant negative CREB transgene inhibits the acquisition of long-term memory, whereas induction of CREB expression enhances memory formation (Yin et al., 1994, 1995). Targeting of α and δ CREB isoforms disrupt long-lasting LTP and long-term associative and spatial memories, whereas acquisition and short-term memory are normal in CREB mutant mice. These studies indicate that CREB-dependent transcription is essential for long-lasting synaptic plasticity and memory but

not for short-term memory (Bourtchuladze et al., 1994). CREB is required for some forms of emotional memory and specifically for the consolidation of long-term conditioned fear memories, but not for encoding, storage or retrieval of these memories (Kida et al., 2002). Disruption of CREB-mediated transcription blocks both reconsolidation and long-term extinction of contextual fear memory, which are associated with reduced levels of the CREB target gene *Arc* in hippocampus and amygdala (Mamiya et al., 2009).

3.2.4 CREB-dependent target genes

There are more than 4000 known genes involved in synapse function, neuronal survival and memory containing in their promoter potential CRE binding sites (Murphy et al., 1991; Cohen and Greenberg, 2008; Lonza and Ginty, 2002). In response to different stimuli, CREB promotes the transcription of genes in minutes (immediate gene expression) and last for few hours (long-term genes) (Tischmeyer and Grimm, 1999). The immediate expression of genes is regulated by CREB and transcriptional coactivators factors or other DNA binding proteins which facilitates subsequent transcription. The following neural genes are regulated by CREB.

Arc

Arc, for activity-regulated cytoskeleton-associated protein (also known as Arg3.1), is a plasticity protein first characterized in 1995. *ARC* / *Arg 3.1* encode a novel cytoskeleton-associated protein in dendrites of post-synaptic of glutamatergic neurons and belong to the immediate-early gene (IEG) family, a rapidly activated class of genes (Lyford et al., 1995).

The presence of the CRE-binding sequence in the promoter of the *Arc* has been described (Kawashima et al., 2009). A number of promoter and enhancer regions have been identified that mediate activity-dependent *Arc* transcription, including a synaptic activity response element (SARE) sequence at ~7 kb upstream that contains binding sites for CREB, myocyte enhancer factor2 (MEF2), and serum response factor (SRF)

(Kawashima et al., 2009). *Arc* is localized to activated synaptic sites in an NMDA receptor-dependent manner (Steward et al., 2001). Transcription of *Arc* occurred in the nucleus and translocated to activated synapses (Steward et al., 1998). In synapses, *Arc/Arg3.1* protein interacts with dynamin and specific isoforms of endophilin to enhance receptor endocytosis which is necessary for maintaining the regulation of AMPA receptors during synaptic activity (Chowdhury et al., 2006; Song and Huganir, 2002). Changes in *Arc* mRNA and/or protein are correlated with a number of behavioral paradigms including cued fear conditioning, contextual fear conditioning, and spatial memory (Monti, et al., 2006; Huff, et al., 2006; Guzowski, et al., 2000; Guzowski, et al., 2001). Activation of *Arc/Arg3.1* is essential for memory consolidation as *Arc/Arg3.1* knockout mice animals fail to form long-lasting memories for implicit and explicit learning tasks, despite intact short-term memory (Plath, et al., 2006).

c-Fos

c-Fos is a 62 kDa protein with a basic leucine zipper region for dimerisation and DNA-binding and a transactivation domain at C-terminus. c-Fos is a part of a bigger Fos family of transcription factors which includes c-Fos, FosB, Fra-1 and Fra-2 as well as smaller FosB splice variants, FosB2 and deltaFosB2 (Milde-Langosch K, 2005). A variety of stimuli promotes transcription of c-fos. *c-Fos* is generally among the first to be induced after stimulation and hence referred to as an IEG. The activity of c-fos is also regulated by posttranslational modification caused by phosphorylation by different kinases including MAPK, cdc2, PKA or PKC.

The expression of c-fos is induced quickly in response to neurotransmitters after the memory test (Graham and Gilman, 1991). The Morris water maze study showed that the peak expression of c-fos was occurred 10 minutes after the completion of the test and the induction is maintained throughout the training (Guzowski et al., 2001). Different memory tests lead to the expression of c-fos in the hippocampus of animals. Adult mice lacking c-fos in the CNS (c-fosDeltaCNS) showed normal general and emotional behavior but were specifically impaired in hippocampus-dependent spatial and

associative learning tasks. These learning deficits correlated with a reduction of long-term potentiation (LTP) in hippocampal CA3-CA1 synapses (Fleischmann et al., 2003).

Nr4a gene family

The NR4A family of transcription factors is a part of the nuclear receptors (NR) superfamily. The structure of nuclear receptors is characterized by an amino-terminal A/B region containing the activation function (AF)-1 transactivation domain, a highly conserved DNA-binding domain (DBD), and a carboxy-terminal ligand-binding domain (LBD) (Figure 12). However, as NR4A proteins have no known ligand, they are described as orphan nuclear receptors. The major difference between NR4A and classic nuclear receptors is ligand-independent regulation, and activity of the NR4A is regulated at the level of gene expression and protein stability (Hawk and Abel, 2011).

Three members of the NR4A family have been identified in mammals: Nur77 (*NR4A1*), Nurr1 (*NR4A2*) and Nor 1 (*NR4A3*) (Law, et al., 1992; Milbrandt, et al., 1988; Ohkura, et al., 1994). All three genes can be expressed in areas CA1 and CA3 of the hippocampus, although the relative abundance in these areas differs for the three genes (Xiao, et al., 1996; Hawk and Abel, 2011). The *Nr4as* are IEG and can be induced by a variety of stimuli, including activation of G-protein-coupled receptors, tyrosine receptor kinases and direct activation of intracellular protein kinase pathways. In addition to regulation of *Nr4a* gene expression, signaling molecules involved in long-term memory formation such as PKA and MAPK also regulate the subcellular localization and activity of newly synthesized NR4A proteins (Hawk and Abel, 2010; Hawk and Abel, 2011).

Recently, several studies show that *Nr4as* may participate in memory formation. Training in the contextual fear conditioning increases expression of Nr4a1 in CA1 hippocampus (Malkani and Rosen, 2000; von Herten and Giese, 2005), an effect that is blocked by reducing CaMKII signaling (Irvine, et al., 2005; von Herten and Giese, 2005; Hawk and Abel, 2011). The expression of Nr4a1, Nr4a2 and Nr4a3 is increased after learning. Blocking NR4A activity in memory-supporting brain regions, including in the hippocampus, impairs hippocampus-dependent long-term contextual fear memory but does not impact short-term memory or hippocampus-independent cued fear memory

(Hawk et al., 2012). In addition, mice with reduced Nurr1 expression are deficient in the retention of emotional memory (Rojas et al., 2007).

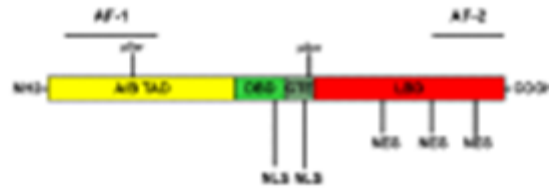


Figure 12. NR4A primary protein structure

NR4A consists of an amino (NH₂)-terminal A/B transactivation domain (TAD) that includes the activator function (AF)-1 region implicated in coactivator recruitment. The DNA-binding domain (DBD) and C-terminal extension (CTE) both contribute to target sequence specificity and contain nuclear localization signals (NLS) that regulate the nuclear import of NR4A proteins. The carboxy (COOH)-terminal ligand-binding domain (LBD) contains the AF-2 domain and three putative nuclear export sequences. Phosphorylation sites (pSer) on NR4A proteins regulate nuclear-cytoplasmic shuttling and DNA-binding capacity. (Hawk JD and Abel T, 2011)

3.2.5 Role of CREB signaling in AD

Bioinformatic analysis of gene expression profile databases have revealed a global deregulation of the CREB transcriptional network associated with AD clinical stages (Sato et al., 2009). It has been reported that as a result of reduced cAMP and PKA activity CREB phosphorylation is reduced in AD brains (Yamamoto-Sasaki et al., 1999). Deficiencies in CREB phosphorylation induced by A β 42 have been associated to deregulated cAMP/PKA signaling (Tong et al., 2001; Vitolo et al., 2002) and altered glutamatergic transmission in neurons (Snyder et al., 2005). Importantly, decreased expression of CREB downstream genes, such as BDNF, c-fos and Egr-1/Zif268, has been observed in hippocampus and frontal cortex of AD brains and APP transgenic mice

(Phillips et al., 1991; Ferrer et al., 1999; Dickey et al., 2003; Plopp et al., 2003). Furthermore, it has been shown that altered CREB signaling is associated with altered NMDA currents and LTP, memory loss and neurodegeneration in *PS1* cDKO mice (Saura et al., 2004).

Taken together, these results suggest that $A\beta$ may alter CREB transcriptional activation, causing deficiencies in synaptic plasticity and memory. Due to its essential role on synaptic plasticity, memory and neuronal survival, it has been proposed that CREB activation may be an alternative therapeutic approach for the treatment of dementia disorders (Tully et al., 2003). The phosphodiesterase IV (PDE4) inhibitor rolipram, which increases cAMP and activates CREB, enhances LTP and associative and spatial memories in old mice (Bach et al., 1999; Barad et al., 1998; Villiger and Dunn, 1981), in a mental retardation mouse model of Rubinstein-Taybi syndrome (Bourtchouladze et al., 2003) and APP/PS1 transgenic mice (Gong et al., 2004).

3.2.6 CREB regulated transcriptional coactivators (CRTCs)

3.2.6.1 CRTC family members

CREB regulated transcription coactivators (CRTCs) are involved in the regulation of CREB-dependent gene expression programs (Conkright, et al., 2003). CRTCs promote the transcription of CREB target genes following its recruitment to promoter regions and by enhancing the interaction of CREB with the RNA polymerase component TAF_{II} 130. CRTCs mediate selective expression of CREB target genes in response to cAMP Ca^{2+} signals, but not by stress stimuli, through interactions with CBP/p300 and increasing its association to specific gene promoters (Wang et al., 2010). In addition to its function on transcription, CRTCs regulate alternative mRNA splicing of certain CREB target genes via a conserved Pro-rich domain, suggesting that they play multiple roles in gene regulation (Amelio et al., 2009). Decreasing CRTC1 level or blocking the interaction between CRTC1 and CREB disrupt CRE-mediated transcription in cultured neurons (Kovács KA et al., 2007, Ch'ng et al., 2012).

Three members of the CRTC family involved on CREB activation named *CRTC1* (mouse *Crtc1*), *CRTC2* (mouse *Crtc2*) and *CRTC3* (mouse *Crtc3*) have been described in mammals (Iourgenko et al., 2003; Ravnskjaer et al., 2007). All three members share the similar modular structures: an N-terminal CREB-binding domain (CBD), a central regulatory (REG) domain, a splicing domain (SD) and a C-terminal Trans-activating domain (TAD) (Figure 13). *CRTC1* is expressed at low levels in the embryonic brain, whereas it is highly expressed in postmitotic neurons of the cortex and hippocampus particularly in early postnatal days (Lisè et al., 2009). All three CRTC isoforms are widely expressed in the forebrain, although *CRTC1* is highly expressed in almost all brain regions including cortex, hippocampus, striatum, thalamus, hypothalamus and other structures (Watts et al., 2011). In contrast to the

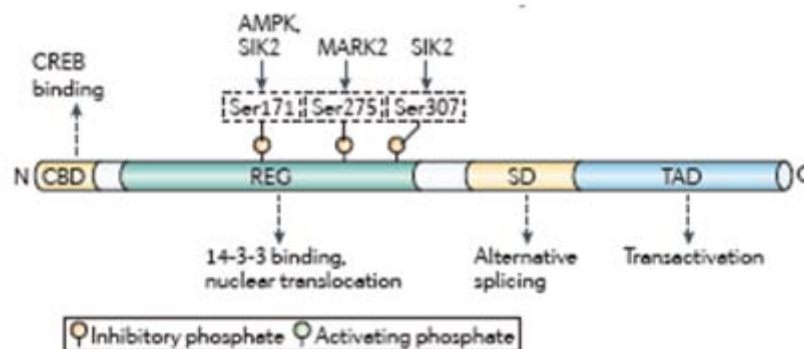


Figure 13. Modular structure of CRTCs

Domain structure of the CRTC family of CREB co-activators, as exemplified by *CRTC2*. CRTCs contain an N-terminal CREB binding domain (CBD), a central regulatory region (REG), a splicing domain (SD) and a C-terminal TAD. CRTC phosphorylation at Ser171 (by AMPK and SIK2), Ser275 (by microtubule affinity-regulating kinase 2 (MARK2)) and Ser307 (by SIK2) promotes 14-3-3 protein binding and the cytoplasmic sequestration of *CRTC2*. (Altarejos J.Y. and Montminy M. 2011).

high levels of *CRTC1* in the brain, *CRTC2* and *CRTC3* are reduced and more sparsely distributed across the forebrain with the exception of some discrete areas, and particularly the hippocampus, PVH, supraoptic, suprachiasmatic, ventromedial nuclei and the piriform cortex (Watts et al., 2011).

In basal conditions, CRTCs are present in the cytosol as phosphorylated forms. cAMP and calcium cause the calcineurin-mediated dephosphorylation and nuclear translocation of CRTCs. Exposure to cAMP and calcium, triggers the calcineurin-mediated dephosphorylation and nuclear translocation of CRTCs, which then bind to CREB over relevant promoters. Indeed, CRTC nuclear transport is sufficient to activate CRE-dependent transcription (Bittinger et al., 2004, Figure 14). Similarly, CRTCs are exported from the nucleus to the cytoplasm through a CRM1-dependent pathway, because treatment with Leptomycin B, an inhibitor of CRM1-mediated protein nuclear export, results in nuclear CRTC accumulation (Bittinger et al., 2004). Nuclear accumulation of CRTC1 is a sensitive readout of synaptic activity in hippocampal neurons. Recent studies show that CRTC1 localizes to dendrites and spines in hippocampal neurons, and translocates to the nucleus in a calcium- and calcineurin-dependent manner following glutamatergic synaptic transmission. CRTC1 is specifically transported from stimulated-synapses to the nucleus only in excitatory neurons which means CRTC1 nuclear accumulation is tightly coupled to stimulation and this transcription factor remains localized in the nucleus as long as excitatory synaptic activity or cAMP levels remain elevated. (Ch'ng et al., 2012). Thus, nuclear CRTC1 is a sensitive monitor of synaptic and neuromodulatory activity that dynamically informs the nucleus about activity received at synapses. Because the nuclear translocation does not require any transcription or translation, it is also a very rapid marker of activity.

CRTC1 expression is almost exclusively confined to the CNS, where it mediates, among others, effects of hormonal and nutrient signals on energy balance-(Altarejos and Montminy, 2011). Thus, *Crtc1* null mice are hyperphagic, obese, and infertile. Active *Crtc1* stimulates the expression of Cocaine and Amphetamine Regulated Transcript (CART) and KISS1 genes, which encode hypothalamic neuropeptides that mediate leptin effects on satiety and fertility (Altarejos et al., 2008). Both the rhythmic and light regulate CRTC1 and CRTC2 in the murine suprachiasmatic nucleus (SCN). In the middle of the day, *Crtc1* expression can be detected in the dorsoventral extent of the SCN, while in the early night, limited expression of CRTC1 can be detected, and during the late night CRTC1 expression levels are between mid-day and early night levels. In contrast to CRTC1, CRTC2 expression has been detected during the day and night. In addition, light

pulse cause CRTC1 nuclear accumulation but not affect CRTC2 subcellular localization (Sakamoto K et al., 2013). The analysis in SCN has found that an entraining stimulus causes *Crtc1* nuclear translocation and acts as a coactivator of CREB-driven transcription of *Sik1* and *Per1*. SIK1 then inhibits further expression of *Per1* by deactivation of CRTC1 (Jagannath, et al., 2013).

CRTC2, the most highly expressed member of this family in the liver, is regulated through phosphorylation by members of the cAMP-activated protein kinase (AMPK) family of stress- and –energy sensing Ser/Thr kinases. CRTC2 is mainly participates in the regulation of gluconeogenic enzymes in the liver and glucose homeostasis (Conkright, et al., 2003). CRTC3 has been less studied but it is known to be present in the liver where it regulates mitochondrial biogenesis and to attenuate beta-adrenergic signaling in adipocytes (Than T. et al., 2011).

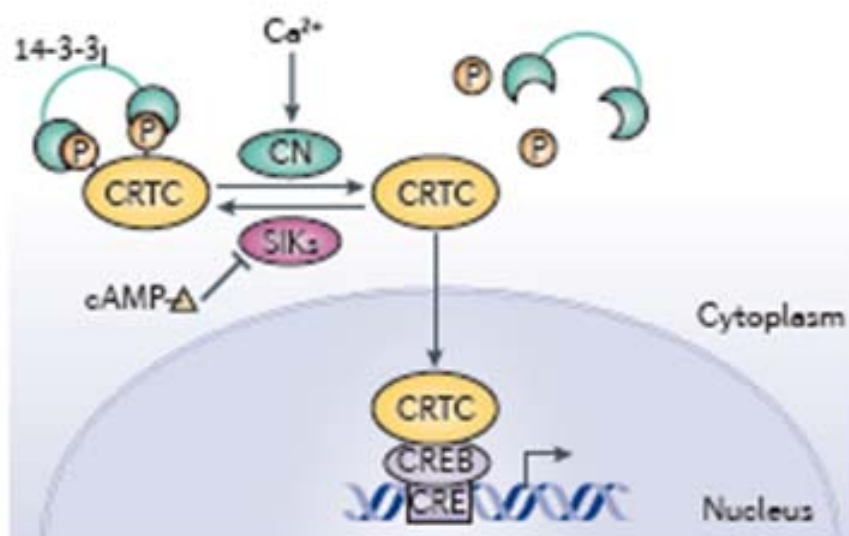


Figure 12. CRTC nuclear shuttling is regulated by phosphorylation
cAMP and calcium signals regulate CREB target genes by stimulating the nuclear translocation of CRTCs. (Montminy, 2011)

3.2.6.2 Role of CRTTC1 in learning and memory

Several studies have shown that CRTTC1 contribute to learning and memory processes. Expression of a dominant-negative form of CRTTC1 (TORC-DN-EGFP-11R) in CA1 neurons blocks the transcription-independent late-phase of long-term potentiation (LTP), but not the early, transcription-independent phase (Zhou et al., 2006; Kovács et al., 2007). In contrast, overexpression of CRTTC1 in CA1 neurons decreases the threshold for late-phase LTP (Zhou et al., 2006). These findings support a critical role of CRTTC1 during hippocampal synaptic plasticity. Moreover, CRTTC1 facilitates fasting-mediated appetitive long-term memory in *Drosophila* (Hirano et al., 2013), and overexpression of CRTTC1 enhances fear memory consolidation (Sekeres et al., 2012). In addition, altered expression of Crtc1-dependent CREB target genes is associated with spatial memory impairments in a transgenic mouse model of AD (España J, 2010). Indeed, genome-wide transcriptome analysis in the mouse hippocampus have recently revealed deregulation of a gene network related with neurotransmission, synaptic plasticity, and learning/memory in the hippocampus of APP_{Sw,Ind} mice after spatial memory training (Parra-Damas A, 2014). Importantly, APP_{Sw,Ind} mice show changes on a CREB-dependent transcriptional program dependent on the Crtc1 likely by reducing Crtc1 dephosphorylation at Ser151. A denoviral-mediated Crtc1 overexpression in the hippocampus of APP_{Sw,Ind} mice efficiently reverses Aβ-induced spatial learning and memory deficits by restoring a specific subset of Crtc1 target genes (Parra-Damas A, 2014). Aβ suppress Crtc1-dependent gene transcription in response to cAMP and Ca²⁺ signals through reduction of calcium influx and P2B/calcineurin-dependent Crtc1 dephosphorylation at Ser151. Expression of Crtc1 or active Crtc1 S151A reverse the deficits on Crtc1 transcriptional activity in APP_{Sw,Ind} neurons.

Whereas the function of Crtc1 on neuronal morphology and plasticity is well established, its role as a mediator of activity-dependent gene transcription required for different forms of memory remain largely elusive. The present study attempts to elucidate the molecular and cellular mechanisms underlying Crtc1 activation during associative

learning and memory in order to clarify the role of Crtcl in associative memory impairments during neurodegeneration.

Objectives

Objectives

1. To study the molecular mechanisms regulating Crtc1-dependent signaling during associative memory in mouse models of neurodegeneration
2. To examine the role of Crtc1-dependent gene transcription during associative memory
3. To study the function of Crtc1 on synapses in mouse models of neurodegeneration

Materials and methods

5 Materials and Methods

Antibody index

Table 1. Primary antibodies used for biochemical analysis

Antibodies	Source	Ref.	Applications
CRTC1	Cell Signaling	#2587	IF 1:300, WB 1:10000
CREB	Cell Signaling	#9197	WB 1:1000
MAP2	Sigma	M1406	IF 1:300
Myc (A-14)	Santa Cruz	sc-789	IF 1:1000, WB 1:500
NeuN	Neuroscience	MAB377	IF 1:1000
pCREB	Cell Signaling	#9198	WB 1:1000
pCRTC1	Saura's lab		

Table 2. Secondary antibodies used for biochemical analysis

Antibodies	Source	Ref.	Applications
Anti-rabbit- Alexa488	Molecular Probes	A-11001	IF 1:200
Anti-rabbit- Alexa568	Molecular Probes	A-11011	IF 1:200
Anti-rabbit- Alexa594	Molecular Probes	A-11012	IF 1:200
Anti-mouse- Alexa488	Molecular Probes	A-10667	IF 1:200
Anti-mouse- Alexa568	Molecular Probes	A-11004	IF 1:200
Anti-mouse- Alexa594	Molecular Probes	A-21044	IF 1:200

Anti-rabbit-HRP	Cell signaling	7074	WB 1:3000
Anti-mouse-HRP	Sigma Aldrich	A3673	WB 1:3000
β -tubulin	Sigma	T7816	WB 1:20000
GAPDH	Ambion Life Technologies	AM4300	WB 1:100000
(Lamin B1)	Zymed	33-2000	WB 1:500

5.1 *In vivo* experimental procedures

5.1.1 Transgenic mice

The generation of PS cDKO mice was described previously (Saura et al., 2004). Briefly, PS1 cKO; PS2^{+/-} (fPS1/fPS1; CaMKII α -Cre; PS2^{+/-}) females (Yu et al., 2004) were crossed with fPS1/fPS1; PS2^{-/-} males (Steiner et al., 1999) to generate control (fPS1/fPS1; PS2^{+/-}), PS1 cDKO (fPS1/fPS1; CaMKII α -Cre; PS2^{+/-}), PS2^{-/-} (fPS1/fPS1; PS2^{-/-}) and double PS cDKO (fPS1/fPS1; CaMKII α -Cre; PS2^{-/-}) mice. Genetic background of all mice was C57BL6/129 hybrid. Animal experimental procedures were supervised and approved by Animal Care and Ethical Committee of the UAB (protocol CEEAH 1783, Generalitat Catalunya 6381) following the European Union guidelines.

Genotyping

Genomic DNA purification: Genomic DNA was purified from a tail piece (1-2 mm) treated with 0.1 mg/ml proteinase K (Roche) dissolved in 0.5 ml of DNA purification lysis buffer, and incubated overnight at 56 °C under stirring for protein digestion. After centrifugation at 12000 rpm for 5 min, genomic DNA was precipitated with 0.5 ml isopropanol (Baker). The

sample was centrifuged at 12000 rpm for 10 min. 0.5 ml ethanol 70% were added to the DNA pellet. After reprecipitation by centrifugation, the pellet was resuspended in 50-100 ml TE buffer, and dissolved at 65 °C 2 h under stirring. DNA was stored at 4 °C.

DNA amplification by Polymerase Chain Reaction (PCR): 2 µl of purified genomic DNA was added to 2.5 µl of PCR buffer (Biotools), 0.5 µl 10 mM dNTP (Biotools), 0.5 µl MgCl₂ 50 mM (Biotools), 0.2 µl Taq DNA polymerase 5 U/ml (Biotools) and forward and reverse primers 0.5 µM (Table 3) in a final volume of 25 µl. The amplification was carried out in a PEXE 0.2 thermal cycler (Thermo Electron Corporation) with the certain PCR profile (Table 4). 15 µl of PCR product was resolved on a 2.5% agarose gel to visualize the amplified bands, using SYBR-Safe (Invitrogen) under UV light

Table 3. Primer used for DNA amplification by conventional PCR and amplified band sizes..

Gene	Name primer/sequence	Size (bp)
<i>fPSI</i>	P139: 5'GGTTTCCCTCCATCTTGGTTG 3'	<i>PSI</i> allele 216bp
	P140: 5' TCAACTCCTCCAGAGTCAGG 3'	<i>fPSI</i> allele 262bp
	P158: 5' TGCCCCCTCTCCATTTTCTC 3'	
<i>PS2</i>	P162: 5' CATCTACACGCCCTTCACGG 3'	<i>PS2</i> 540 bp <i>ΔPS2</i> 326 bp
	P163: 5' CACACAGAGAGGCTCAAGATC 3'	
	P164: 5' AAGGGCCAGCTCATTCTCC 3'	
<i>CaMKIIα-Cre</i>	P156: 5' GCCTGCATTACCGGTCGATGCAACGA 3'	WT no band <i>CaMKIIα-Cre</i> 700 bp
	P157: 5'GTGGCAGATGGCGCGCAACACCATT 3'	

Table 4 PCR procedure for a mplification of *PS1*, *PS2* and *CaMKII-Cre*

Gene	<i>PS2</i>	<i>PS1</i> , <i>CaMKII-Cre</i>
PCR Profile	94°C, 4 min 94°C, 1 min 65°C, 1 min 72°C, 1 min 72°C, 7 min 4°C, forever	94°C, 4 min 94°C, 1 min 60°C, 1 min 72°C, 1 min 72°C, 7 min 4°C, forever

5.1.1 Injection of recombinant AAVs

Adeno-associated virus (AAV2/10) from rhesus macaque (AAVrh.10) containing AAV2 genome into AAV10 packaging vectors is specific for neuron transduction (Klein et al., 2008). AAV2/10-Crtc1-myc was generated by subcloning pDNA3-Crtc1-myc (Kovacs et al., 2007) into pVAX1 (Invitrogen) and pGV-IRES2-GFP vectors. AAV were generated by transfecting HEK293T cells with AAV2 recombinant, pRepAAV2/CapAAV10, and pXX6 vectors. For viral injections, 6-month old mice (=8 mice/group) were anesthetized with isoflurane and placed in a stereotaxic platform (Kopf). The injection coordinates for the hippocampus were as follows: anterior 0.2 caudal to bregma; 0.18 lateral to bregma; depth 0.2 ventral to dural surface according to (Paxinos and Franklin, 2004). AAV2/10-GFP or -Crtc1 viral stocks (3 μ l; 5.1×10^{11} gc/ml; 0.5 μ l/min) were injected bilaterally into the hippocampus.

5.1.2 Behavior

Mice used for behavioral studies were handled individually for 3 min during three consecutive days. For contextual fear conditioning, mice were placed within the conditioning chamber (15.9 x 14 x 12.7 cm; Med Associates Inc., St. Albans, VT) for 3 min in (*neophobia freezing*) to allow them to develop a representation of the context via exploration before the

onset of the unconditioned stimulus (footshock; 1s/1mA). After the shock, they were left in the chamber for 2 min (*immediate freezing*) and returned to the home cages. Conditioning was tested 2 h (*short-term*) or 24 h (*long-term*) after training for 4 min in the same conditioning chamber. The control *context group* remained in the chamber for 5 min and did not receive footshock, whereas the *shock group* received footshock and immediately returned to the home cage to eliminate the association of context and unconditioned stimulus. Mice were sacrificed by dislocation 15 min, 2 h or 24 h after training. Freezing, defined as a complete cessation of all movement except for respiration, was analyzed automatically by using the *Video Freeze Software* (Med Associates, Inc.).

5.1.3 Intracardial perfusion and histology

Paraffin sections

Mice were anesthetized with a lethal pentobarbital dose (120 mg/kg) and perfused intracardially with 0.9% NaCl solution and fixed with 4% formaldehyde for 10 min. Brains were removed and immersed in 4% formaldehyde for 2 h. Tissue was dehydrated in a graded series of ethanol followed by xylene and then embedded in paraffin. Brain was sectioned at 5 μm and mounted on glass slides. Sections from each genotype were mounted on the same slide in order to achieve maximum homogeneity during staining procedures.

Floating sections

Mice were anesthetized with a lethal pentobarbital dose (120 mg/kg) and perfused intracardially with 0.9% NaCl solution and fixed with 4% formaldehyde for 10 min. Brains were removed and immersed in 4% formaldehyde for 2 h. Then brain was transferred to 30% sucrose in PB buffer overnight. The tissue was freeze and sectioned at 40 μm thickness in cryostat (Leica C M 3050s). The sample was kept in antifreezing buffer at -20 $^{\circ}\text{C}$.

Solution

PB buffer (0.1 M, pH 7.4): Mix NaH_2PO_4 2.70977g and Na_2HPO_4 10.9898g to 1L and check the pH.

Antifreezing Buffer: PB 0.1 M pH 7.4 30ml, Ethylene glycol 40 ml, Glycerol 30 ml.

5.2 Human brain tissue

Human brain samples were obtained from brain banks of Hospital de Bellvitge (Universitat de Barcelona, Spain) and Fundació CIEN (Instituto de Salud Carlos III, Spain). Brain samples were matched as closely as possible for sex, age and postmortem interval (Table 5). Neuropathology was classified according to Braak staging for neurofibrillary tangles and neuritic plaques according to previous reported protocols (Braak et al., 2006).

Table 5. Summary of human brain samples used in the biochemical assays

Braak stage	n	Sex	Age	PMD (h)
Ctrl	12	4F/8M	50,42 ± 2,34	6,33 ± 0,69
I-II	12	2F/10M	68,58 ± 2,74	6,75 ± 1,25
III	5	2F/3M	76,80 ± 3,31	8,55 ± 2,35
IV	5	2F/3M	85,40 ± 3,87	7,12 ± 2,74
V-VI	8	4F/4M	78,63 ± 2,37	9,71 ± 2,09

F, Female; M, male; PMD, postmortem delay;

5.3 Cell culture**5.3.1 Primary neuronal culture**

Both hippocampal and cortical neurons were obtained from E15 mouse embryos. After embryo decapitation, brain was extracted, the hemispheres were separated and meninges were discarded to avoid the

presence of fibroblasts. Cortices or hippocampi were dissected and incubated with filtered Krebs buffer (solution 1) previously filtered. Tissue was centrifuged with solution 1 (250 x g, 30 sec), the pellet was incubated with trypsin (solution 2) to disgregate enzymatically the tissue at 37 °C for 10 min. Solution 4 was added to inhibit trypsin activity and DNA degradation. Tissue was centrifuged (250 x g, 30 sec), the supernatant was discarded and the pellet was incubated with solution 3. Then this solution was digested mechanically using a Pasteur pipette. To obtain a cellular suspension, it was filtered through a nylon mesh (diameter 40 µm) to eliminate the cell clumps. The suspension was transferred to a tube with solution 5 and the cells were centrifuged at 1000 rpm for 5 min. The supernatant was discarded and the pellet containing the cells was resuspended in seeding medium. Cell number was obtained by using a Neubauer chamber.

Cells in DMEM were seeded on 24 well-dished (50,000 cells/well for immunocytochemistry; 100,000 -150,000 cells/well for luciferase assay) or on 6-well dishes (350000 cells/well for biochemical assays). Two hours after incubation at 37°C and 5% CO₂, seeding medium was removed Neurobasal medium containing 2% B27, 2 mM glutamine and 30 mM glucose was added. Cells were washed and processed for immunofluorescence, used for luciferase assays or lysed for biochemical analysis.

Solution

Dulbecco's Modified Eagle Medium, DMEM (Sigma Aldrich D5796)

Neurobasal (Gibco, 21103-049)

Fetal Bovine Serum, FBS (Invitrogen-Gibco 10106-169)

Bovine serum albumin (Sigma T4665)

B27 (Invitrogen 17504-044)

Poly-D-lysine (Sigma P7658)

Trypsin (Sigma T4665)

Trypsin inhibitor (Sigma 17075-029)

Solution 1: 120 mM NaCl, 4.8 mM KCl, 1.2 mM KH_2PO_4 , 25 mM NaHCO_3 , 14.3 mM Glucosa, 0.3% bovine serum albumin and 0.03% Mg_2SO_4

Solution 2: Solution 1, 0.025% trypsin

Solution 3: Solution 1 plus 0.052% trypsin inhibitor, 0.008% DNase and 0.03% MgSO_4

Solution 4: Solution 1 plus 16% solution 3

Solution 5: Solution 1 plus 0.03% MgSO_4 and 0.0014% CaCl_2

5.3.2 PC12 culture and differentiation

Cell plates were coated with Collagen (BD 354236). Collagen was 1:50 diluted and added 2 ml in to the wells of a 60 mm dish at room temperature for 1 h and washed with ddH₂O. PC12 cells were plated in complete medium. 100 ng/ml NGF was added in to media 24 h later, and the NGF was renewed every 2 days. PC12 cells were transfected 4 days after NGF treatment. 24 h later the cell were stimulated and lysis for CRE-transcriptional activity analysis.

Solution

Completed medium: 500 ml DMEM (Sigma D5796) with glutamine, 35 ml FBS, 35 ml HS, 1 ml AB, 5.75 ml HEPES 1M, pH6.8.

5.3.3 Transfection and shRNA

Transfection of primary neurons

CRE-luciferase and TKRenilla plasmids were obtained from Stratagene and Promega, respectively.

Lipofectamine 2000 reagent was used for transfection of hippocampal and cortical neurons. Lipofectamine 2000 is a cationic liposome formulation that functions by complexing with nucleic acid molecules, allowing them to overcome the electrostatic repulsion of the cell membrane and to be taken up by the cell. 1 μl of Lipofectamine 2000

was diluted in 50 μ l OptiMEM containing 1mM glutamine, a solution that was incubated at room temperature for 5 min. 1-2 μ g DNA were mixed with 50 μ l OptiMEM containing 1mM glutamine, incubated at room temperature for 20 min.

100 μ l OptiMEM containing DNA/Lipofectamine 2000 transfection complexes were added to each well, containing approximately 200 μ l of medium. The transfection medium was incubated for 2 hours at 37 °C. Before replacing the conditioned culture medium kept at 37 °C was added again to the well.

Solution

Lipofectamine 2000 reagent: Invitrogen 11668-019

OptiMEM: Invitrogen 31985-062

Lentiviral infection

Oligonucleotides were cloned into BglIII/HindIII sites of the pSUPER.retro.puro plasmid (OligoEngine). Lentiviral vectors were obtained by digesting EcoRI-ClaI sites from pSUPER-Sh to generate the sequence H1-shRNA that was inserted into pLVTHM vector. Lentiviral particles were generated in HE293T cells transfected with pLVTHM-Sh, pSPAX2, and pM2G vectors.

Cultured neurons were infected at 3-4 DIV. Lentiviral particles were added to the culture medium, which was removed 12 h after infection. In the case of lentiviral Crtc1 shRNAs and scramble shRNA, 1 particle/cell was used, whereas lentiviral Cre-recombinase and lentiviral Δ Cre-recombinase was used at 2 particles/cell.

5.3.4 Pharmacological treatments

For Western blotting, neurons were treated with vehicle or KCl (30 mM) and forskolin (20 μ M) and collected at different time points. For immunocytochemistry (ICC), neurons were treated with vehicle or KCl (30 mM) and forskolin (20 μ M) for 30 min before fixation. For CRE-

transcriptional activity analysis, neurons or PC12 cells were treated with vehicle, KCl (30 mM) and/or forskolin (20 μ M) for 4 h before lysis. SIK inhibitors were added 1 h before stimulation at different concentration as detailed below according to the IC50 (Table 6).

SIK Inhibitor	Final Concentration
MRT 199665	1 μ M
MRT 67307	2 μ M
HG 9-91-01	500 nM
KIN 112	10 μ M
STS	10 nM

Table 6. The concentration of SIK inhibitors used for experiment.

5.4 Biochemical methods

5.4.1 Cell and brain lysis and protein quantification

Mice were scarified by dislocation, and the brain was dissected on ice. Cortices or hippocampi were homogenized with a dounce homogenizer in lysis buffer containing protease and phosphatase inhibitors. 1200 μ l lysis buffer was used for 1/2 cortices and 400 μ l lysis buffer was used for 1/2 hippocampi. Cells were washed twice with ice-cold PBS (1x) and then lysed in cold RIPA lysis buffer containing protease and phosphatase inhibitors (100 μ l/well of 6-well dishes). The lysate was sonicated using 35% of power (relative output 5.5) for 10 sec (Dynatech Sonic Dismembrator model 300), and keep the samples on the ice for at least 25 sec. Protein concentration was determined by the BCA method (Pierce#23225).

Solution

Lysis buffer: 50 mM Tris-HCl, pH 7.4, 150 mM NaCl, 2 mM EDTA, 0.5%

Triton X -100, 1% NP-40, .1% SDS, 1 mM Na₃VO₄, 50 mM NaF, 1 mmol/L PMSF.

RIPA lysis buffer: 50 mM Tris base pH 7.4, 150 mM NaCl, 2.5 mM EDTA, 1% NP40, 0.5% sodium deoxycholate, 0.1% SDS, 1 mM Na₃VO₄, 1 mM PMSF.

Protease inhibitor cocktail tablets: Roche #11836145001

Phosphatase inhibitors: Roche #04906837001

BCA protein assay kit: Pierce 23225

5.4.2 Gel electrophoresis and Western blotting

Equal amount of protein were diluted with sample loading buffer (3x) and heated at 95°C for 5 min before load each sample onto each lane. A molecular weight marker was added to identify the proteins of interest. The density of polyacrilamide gels (PAGE) ranged from 7% -12.5% depending on the protein of interest. Proteins were transferred to methanol-activated PVDF membranes and membranes were stained with Ponceau S solution to verify the presence of transferred protein.

To avoid non-specific protein interactions, PVDF membranes were incubated with blocking solution for 1 hour. After blocking, membranes were washed with TBST (10 min x 3). Membranes were incubated with primary antibody diluted in antibody buffer for 2 h at room temperature or overnight at 4 °C. Membranes were washed with TBST (10 min x 5) followed by incubating with secondary antibody coupled to HRP at room temperature for 45 min. Finally, membranes were washed with TBST (10 min x 5) before chemoluminescence reaction with Western Light plus-ECL.

If necessary, the membrane was stripped in stripping buffer at room temperature for 1h and wash with TBST (10 min x 3) before starting new blotting.

Solution

Sample loading buffer (1x): 62.5 mM Tris HCl pH 6.8, 10% glycerol, 2% SDS, 5% β -mercaptoethanol (β ME) and 0.01% bromophenol blue

SDS-PAGE electrophoresis buffer (10x): 250 mM Tris buffer, 2 M Glycine, 1% SDS, pH 8.3

Transfer buffer (20x): 200 mM Tris base and 2 M Glycine, pH 8.3

TBST: Tris 30.3g, NaCl 80.1g, Tween-20 10 ml, add ddH₂O to 1L, pH 7.6

Blocking solution: 5% skimmed milk powder and 0.05% Tween in TBS, pH 7.4

Primary antibody buffer: 0.1% BSA and 0.02% thimerosal in TBST, pH 7.4

Stripping buffer: 0.1 M Glycine pH 2.3

Ponceau S solution: Sigma 81462

Molecular weight marker: Invitrogen 10748-010

Immun-Blot PVDF membrane for protein blotting: Bio-rad 162-0177

Western Light plus-ECL: Peroxide solution (Promega, #W100B), Luminol enhancer solution (Promega, #W101B)

5.4.3 Dual-luciferase reporter assay

For luciferase reporter assay, 6-14 DIV neurons in 24-well dishes (100000 cells/well) were transfected with pCRE-luc (0.5 μ g), TK-Renilla (0.25 μ g), and empty vector or the indicated plasmids (0.5 μ g) by using Lipofect AMINE 2000. For interference assays, 3-4 DIV neurons were infected with shRNA lentiviral vectors (1 transducing units per cell). Neurons were treated at 7 DIV with the indicated reagents before stimulation with vehicle, KCl (30 mM), and/or forskolin (20 μ M; Sigma) for 4 h. Luciferase activity was measured by triplicate in at least three independent transfections by using the Dual-Luciferase Assay System (Promega E1960) in a Synergy HT luminometer (Bio-Tek, power wave xs).

5.4.4 Immunoprecipitation

For immunoprecipitation, 1 ml lysate (1 mg approx) were precleared with adding 100 μ l of beads slurry (Pierce #22811) followed by end-over-end rotation for 20 min at 4 °C. Centrifuge at 2000 g for 2 min at 4 °C. Discard bead pellet and keep supernatant for immunoprecipitation.

Lysate (500 μ g, 500 μ l) and recommended amount of antibody (2 μ l) were incubated overnight at 4 °C. Add 40 μ l of the beads to each sample and incubated for 2 h at 4 °C. The beads were washed for three times, each time centrifuging at 2000 g for 2 min at 4 °C and removing the supernatant. 1) (1x) lysis buffer, 10 min, 4 °C; 2) (1x) lysis buffer 0.5% NP-40, 10 min, 4 °C; 3) (1x) lysis buffer 0 or 0.1% NP-40, 10 min, 4 °C. 25 μ l 2x loading buffer were added to the samples. Boil at 95 °C for 5 min. The samples were checked by gel electrophoresis and instant blue (Expedeon # ISB1LUK).

5.5 Molecular biology methods

5.5.1 Quantitative RT-PCR

RNA from cultured neurons or hippocampal tissue was isolated using this PureLink RNA Mini Kit according to manufacturer's instructions (Ambion, Life Technologies, USA). The RNA integrity number (RIN) was measured using the Agilent 2100 bioanalyser (Agilent Technologies, USA). Mouse RNA (1 μ g; RIN > 8.0) were reverse-transcribed in 50 μ l of a reaction mix containing 1 μ M of Oligo (dT) primers, 1 μ M random hexamers, 0.5 mM dNTP, 0.45 mM DTT, RNaseOut (10 units) and SuperScriptTM II reverse transcriptase (200 units; Invitrogen) at 25°C for 10 min, 42°C for 60 min and 72°C for 10 min. Quantitative real time RT-PCR of a reaction mix containing 1:20 to 1:100 diluted cDNA (5 μ l), primer pairs designed with PerlPrimer v1.1.14 (Owen Marshall) and the Power SYBR Green PCR Master Mix (15 μ l; Invitrogen) was performed in duplicate using the Applied Biosystems 7500 Fast system. Amplification specificity was assessed by melting curve

analysis and amplification efficiencies were calculated from the fluorescence raw data using the LinRegPCR software (Ruijter et al., 2009). Data analysis was performed by the comparative ΔC_t method using the C_t values and the average value of PCR efficiencies obtained from LinRegPCR software (Ruijter et al., 2009). Gene expression was normalized to *Gapdh* for cultured neurons or the geometric mean of *Gapdh*, hypoxanthine guanine phosphoribosyltransferase (*Hprt*) and peptidylprolylisomerase A (*Ppia*) for brain samples. The stability of the reference genes was evaluated in each experiment using the NormFinder, BestKeeper and geNorm algorithms (Bustin et al., 2009)

5.6 Microscope methods

5.6.1 Immunocytochemistry

Hippocampal and cortical neurons (50000cells/well) were cultured in 24-well dishes containing 12 mm coverslips. After 19-21 DIV were washed with cold PBS and fixed with 4% paraformaldehyde in PBS for 15 min at room temperature. Cells were permeabilized with 0.02% saponin in PBS for 7 min at room temperature and blocked with 10 mM glycine in PBS. Finally, nonspecific protein binding was blocked with 10 mM glycine and 5% BSA in PBS for 1 hour. Cells were incubated with primary antibodies diluted in 1% normal goat serum in PBS overnight at 4 °C.

Cells were washed with PBS (10 min x 3). Secondary antibodies were diluted with 1% normal goat serum in PBS and incubated for 45 min at room temperature. Again, cells were washed with PBS (10 min x 3). Hoechst staining was performed by incubating the cells for 5 min at room temperature. After extensive washes with PBS (10 min x 3), coverslips were mounted in slides using FluorSave Reagent (Calbiochem). Cells were examined with a Nikon Eclipse i90 fluorescence microscope or a Leica laser confocal microscope TCSSP5.

Solution

PBS (10X): 80 g NaCl, 2.2 g KCl, 18.680 g $\text{Na}_2\text{HPO}_4 \cdot 7\text{H}_2\text{O}$, 2.0 g K_2HPO_4 , pH 7.4

5.6.2 Immunohistochemistry

Paraffin sections

Coronal brain sections were heated at 60 °C for 2 h. Paraffin was removed by immersing the slides in xylene (twice, 5 min) followed by rehydration in a graded series of ethanol (100%, 100%, 95%, 70%, 50% and distilled water; 3 min each). Heat-induced antigen retrieval was applied by steaming sections in a microwave at high power for 8 min on citrate solution (1x). After 30 min at room temperature, slides were washed with TBS (1x) and incubated with normal goat serum (NGS; Invitrogen) and 0.02% Triton X-100 in Tris-buffered saline pH 7.6 for 30 min, followed by overnight incubation at 4 °C with primary antibodies. The next day, sections were washed with TBS (10 min x3) followed by incubation with the corresponding secondary antibodies in 10% NGS and 0.02% Triton X-100 in TBS at RT for 90 min. Cell nuclei were stained using Hoechst 34580 (1:5000, Molecular Probes). Finally, slides were mounted over coverslips using FluorSave Reagent mounting media (Calbiochem) and analyzed with a laser scanning confocal microscope.

Floating sections

Tissue sections in 0.1M TBS, pH 7.3 were washed with TBS (3 x 5 min plus 3 x 10 min). Sections were incubated at room temperature in gentle stirring for 30 min in blocking buffer. Sections were incubated with primary antibodies diluted in blocking buffer overnight at 4 °C. Wash with TBS 3*10 min. Incubate the sections with secondary antibodies which diluted in TBS for 90 min at room temperature. To visualize the cell nucleus, add 5 µl per well of 1:100 Hoechst from stock (Hoechst stock 1:10000 dilution) half hour before the end of secondary antibodies incubation. Wash with TBS 3*10 min and mounted on slides with

FluorSave Reagent (Calbiochem). The slides were analyzed with a laser scanning confocal microscope.

Solution

TBS: 20 mM Tris base, pH 7.6, 136.87 mM NaCl

TBST: TBS (500 μ l/24-well), 0.2% Triton X-100

Blocking buffer: Normal goat serum 5% in TBST

5.6.3 Nissl staining

The floating sections were left on the slides overnight followed by treated with the graded solution (50% ethanol, 70% ethanol, 96% ethanol, 2x 100% ethanol, 2x xylene, 2x 100% ethanol, 96% ethanol, 70% ethanol, 50% ethanol) for 5min each. Wash the slides with water and stained with cresil violet (5 g/l) for 5 min. After dehydratation (50% ethanol, 70% ethanol, 96% ethanol, 2x 100% ethanol, 5 min for each) and paraffin (xylene 5min twice), sections were mounted into coverslips and analyzed with a Nikon Eclipse 90i microscope.

5.6.4 Image acquisition and processing

Nissl staining was examined using Nikon Eclipse 90i epifluorescence microscope (Nikon Instrument) couples to a DXM 1200F uptake imaging system and ACT-1 software (Nikon).

Immunofluorescence staining was examined using AxioZeiss Examiner D1 LSM700 confocal microscope.

5.7 Statistical analysis

Statistical analysis was performed with GraphPad Prim 5 software, using one-way ANOVA or two-way ANOVA. Data was shown as the mean \pm SEM or SD. Differences with $p < 0.05$ were considered significant.

Results

6.1 Part I : Crtc1 function is critical for contextual memory

6.1.1 Activity-dependent Creb/Crtc1 activation in cultured neurons

To investigate the mechanisms involved in Creb-dependent signaling and transcription in neurons, we first established a neuronal cell line model of PC12 cells, a rat pheochromocytoma cell line commonly employed for studies of neuronal development. PC12 cells cultured in serum-free medium can differentiate to a neuronal phenotype induced by neurotrophic factors. The neurotrophic factor NGF apparently induces a time-dependent morphological differentiation of PC12 cells starting at 2 days (Fig. 1). Cells show 4 days after and already differentiated at 2 days and most cells with morphology of connected fibers at 4 days (Fig. 1). PC12 cells show abundant processes and fiber connections at 4 days of treatment, so at this time point was used for the following experiments.

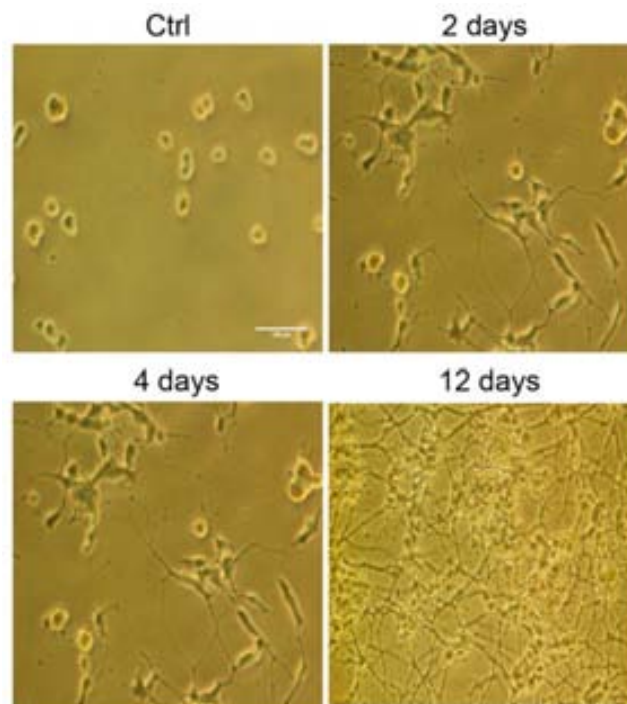


Figure 1. PC12 differentiation.

PC12 cells were treated by NGF and taken the photos at different time points. Scale bar: 100 μ m.

To mimic the effects of neuronal activity, cells were treated with KCl to increase intracellular Ca^{2+} through voltage-gated calcium channels after depolarization or with the adenylate cyclase activator forskolin (FSK) to increase intracellular cAMP levels (Greer and Greenberg, 2008). Treatment with FSK and KCl resulted in ~21- and ~2-fold increase on CRE-luciferase activity, respectively (Fig. 2). In contrast to primary hippocampal or cortical neurons (España et al., 2010), FSK/KCl treatment did not induce a synergistic effect on CRE transcriptional activity (~19-fold) (Fig. 2). Inhibition of calcineurin with cyclosporine selectively blocked CRE-transcriptional activity induced by cAMP/ Ca^{2+} signals (Fig. 2). As the CREB transcriptional coactivators Crtc1 mediate the synergistic effect of cAMP and Ca^{2+} on CREB-dependent transcription (Screaton et al., 2004), we then focused on Crtc1, the most abundant Crtc isoform in neurons and brain (Kovács et al., 2007; Altarejos et al., 2008). Lentiviral vectors expressing Crtc1 shRNA decreased Crtc1 and CRE-mediated transcription induced by cAMP/ Ca^{2+} signals (~40%) (Fig. 2).

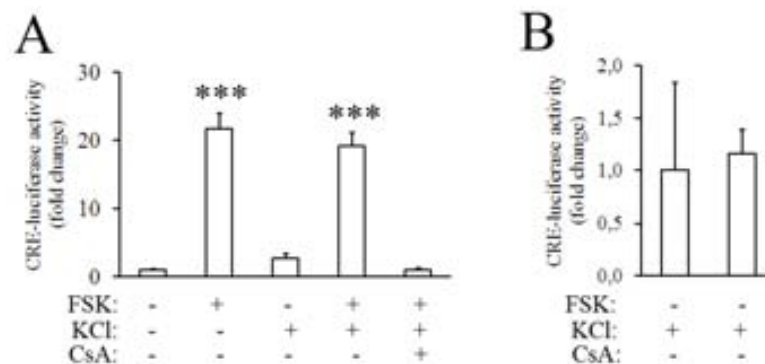


Figure 2. CRE-transcriptional activity in neuronal differential PC12 cells.

PC12 cells were treated by NGF for 4 days and transfected with CRE-luciferase and TK-Renilla plasmids followed by stimulated by FSK/KCl before quantification of luciferase activity. *** $P < 0.000$.

Next, we investigated whether Crtc1 subcellular localization could be regulated by neuronal activity. To achieve this, we performed immunofluorescence staining of Crtc1 in primary neurons. Under basal condition, Crtc1 was enriched in the cytoplasm and highly colocalized with the dendritic marker MAP2. After stimulation with KCl/FSK, Crtc1 translocates to the nucleus decreasing the colocalization with MAP2 (Fig. 3).

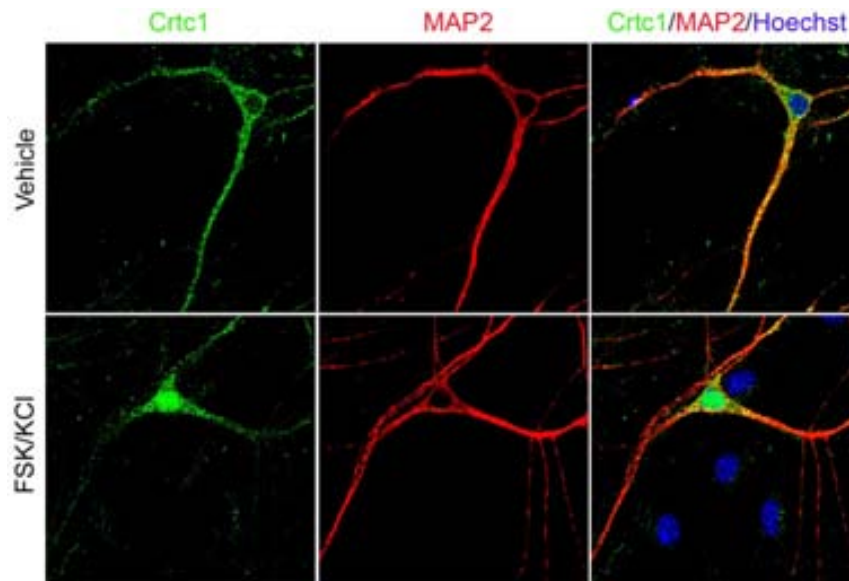


Figure 3. Translocation of Crtc1 to the nucleus in response to neuronal activity.

Representative image of Crtc1 (green), MAP2 (red) and nuclear (Hoeschst 33324, blue) staining in neurons treated with vehicle or FSK/KCl for 15 min.

As Crtc1 was translocated to the nucleus upon neuronal stimulation, we therefore investigated the timing of Crtc1 dephosphorylation, a measure of Crtc1 activation, in primary neurons. Biochemical analysis showed that Crtc1 is rapidly dephosphorylated in response to cAMP/Ca²⁺ signals (Fig. 4). Indeed, Crtc1 was rapidly dephosphorylated already at 1 min after stimulation. Similarly, phosphorylation of Creb at Ser133 was increased at 1 min and reached the peak at 15 min (Fig. 4).

These results suggest that Crtc1 and Creb are quickly activated after

neuronal stimulation, and phosphorylation of Creb get the maximum level at 15 min after stimulation.

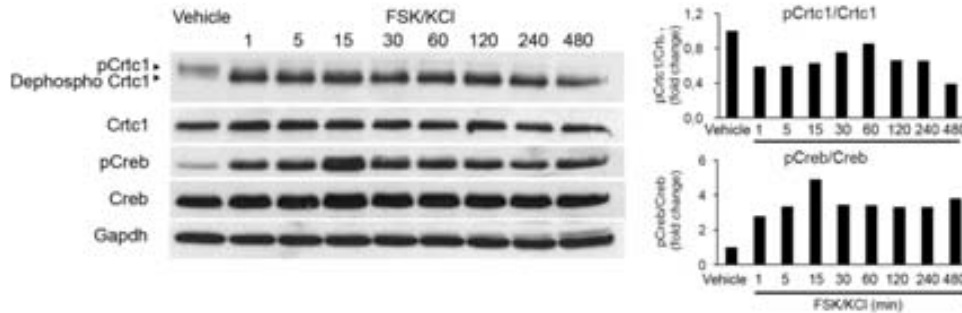


Figure 4. Activity induces changes on phosphorylation of Crtc1 and Creb in cultured cortical neurons.

Western blot (left) and quantification (right) analyses of pCrtc1, Crtc1, Creb and pCreb (Ser133) in cultured cortical neurons stimulated with vehicle or FSK/KCl for 0-8 h. pCrtc1 was decreased after stimulation quickly, while pCreb was increased. Total Crtc1 and Creb protein expression levels were not change.

6.1.2 Contextual learning induces Crtc1 dephosphorylation in the hippocampus

To investigate the specific role of Crtc1 in associative learning we analyzed Crtc1 activation in the hippocampus after contextual fear conditioning (CFC). In this task, context and shock association elicits a fear memory response (i.e freezing) in rodents, whereas single context or shock does not result in fear conditioning to the context (Rosen, 2004). Mice used for behavioral studies were handled individually for 3 min during three consecutive days. For contextual fear conditioning, mice were placed within the conditioning chamber (15.9 x 14 x 12.7 cm; Med Associates Inc., St. Albans, VT) for 3 min (neophobia freezing) to allow them to develop a representation of the context via exploration before the onset of the unconditioned stimulus (footshock; 1s/1mA). After the shock,

they were left in the chamber for 2 min (immediate freezing) and returned to the home cages. Conditioning was tested 2 h (short-term) or 24 h (long-term) after training for 4 min in the same conditioning chamber. Fear conditioning induced a time-dependent increase of freezing responses after training indicating efficient contextual memory association (training effect: $F(3, 42) = 9.26$, $P = 0.0001$), whereas unshocked context-exposed mice did not develop contextual fear memory (Fig. 5).

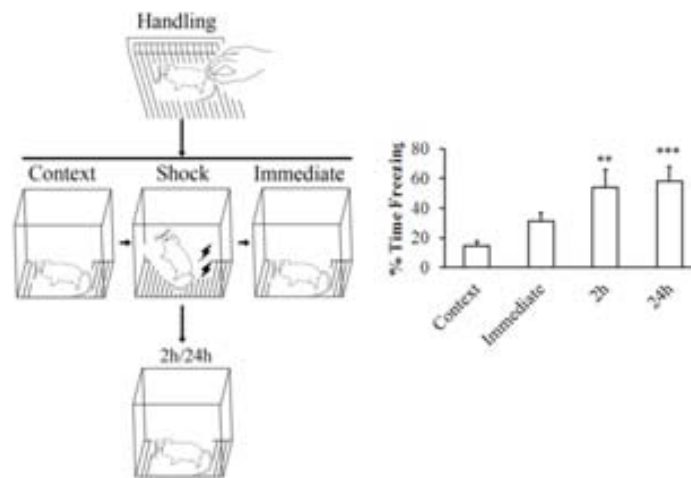


Figure 5. Contextual fear conditioning induces freezing responses in control mice.

Left: Schematic design of the contextual fear conditioning test performed in this study. Different groups of mice were exposed to a novel context without shock (context) or with shock and immediately removed (shock) or remained in the chamber for an additional 2 min and then sacrificed 15 min, 2 h and 24 h after training. Different groups of mice were used for immediate, short-term and long-term. Right: Freezing responses of mice before shock ($n=20$) or immediately ($n=16$), 2 h (short-term; $n=5$) and 24 h (long-term; $n=5$) after contextual training. * $P < 0.05$, ** $P < 0.001$, *** $P < 0.0001$.

Next, we checked whether Creb and Crtc1 protein levels were changed after CFC training. The mice were treated by 1) only handling (naïve), 2) left in the chamber for 5 min without shock (context), 3) only shock (shock), 4) 3 min's contextual exposure followed by shock plus 2 min's contextual exposure and

sacrificed in 15 min after CFC (15 min), 5) sacrificed in 2 h after CFC (2 h) or 6) sacrificed in 2 h after CFC (24 h). Biochemical analyses showed a time-dependent increase of Creb phosphorylation (Ser133) in the hippocampus of mice exposed to a novel context with or without shock (Fig. 6). Notably, contextual learning induced a significant transient decrease of phosphorylated (p) Crtc1 at Ser151 15 min and 2 h after training ($F(4, 16) = 4.34, P = 0.01$), whereas pCrtc1 levels were unchanged by context or shock alone (Fig. 6). Contextual learning did not affect expression of total Creb and Crtc1 ($P > 0.05$; Fig. 6).

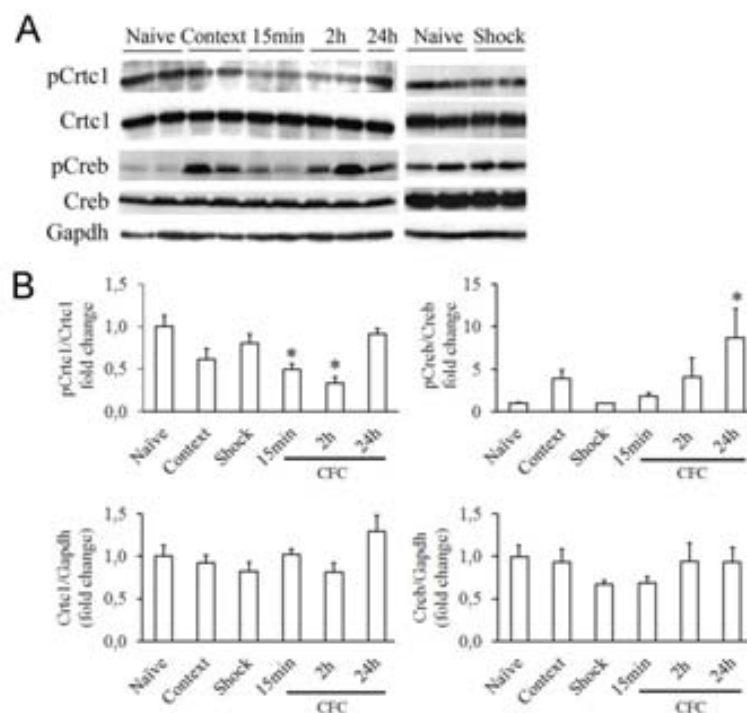


Figure 6. Contextual learning but not novel context induces dephosphorylation of CRTC1 in the hippocampus.

A. Western blot analyses of CRTC1, pCRTC1, CREB and pCREB (Ser133) in the hippocampus of home cage mice (naïve) or mice exposed to training chamber without shock (context) or with shock and sacrificed 15 min, 2 h and 24 h after contextual training. GAPDH was used as loading control. **B.** Quantitative of WB. Values represent fold changes \pm s.e.m ($n = 4-5$ mice/group). * $P < 0.05$.

We next analyzed pCREB and pCrtc1 levels in the cortex by using similar biochemical analysis. In contrast to the hippocampus, levels of phosphorylated Creb or Crtc1 were unchanged in the cortex of context or CFC groups (Fig. 7). These results revealed that contextual learning induces Crtc1 dephosphorylation specifically in the hippocampus, and that Creb is already phosphorylated in the hippocampus after context encoding.

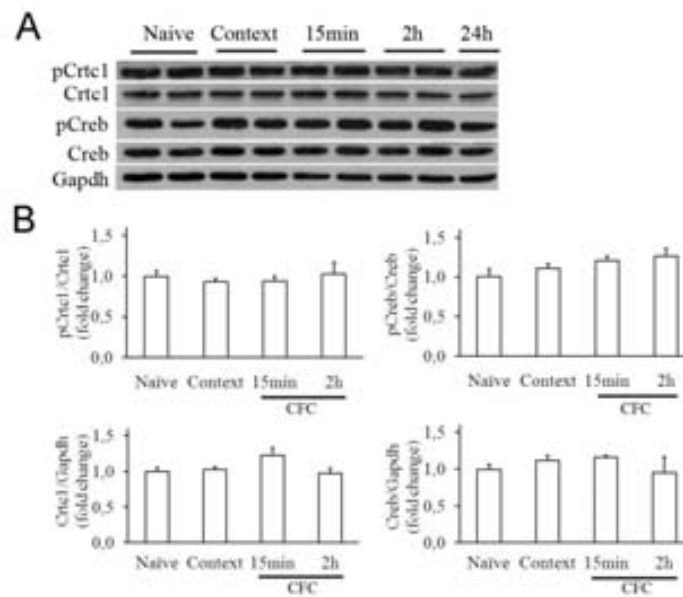


Figure 7. Contextual learning does not affect CRTC1 phosphorylation in the cortex.

A. Western blot analyses of CRTC1, pCRTC1, CREB and pCREB (Ser133) in the cortex of experimental mice used in Fig. 5. **B.** Quantitative of WB. Statistical analysis was determined by one-way ANOVA followed by Dunnett's multiple comparison post hoc test.

6.1.3 Contextual learning induces Crtc1 nuclear translocation in the hippocampus

To examine whether contextual learning induced nuclear translocation of Crtc1 *in vivo*, we analyzed Crtc1 localization in the CA3 and

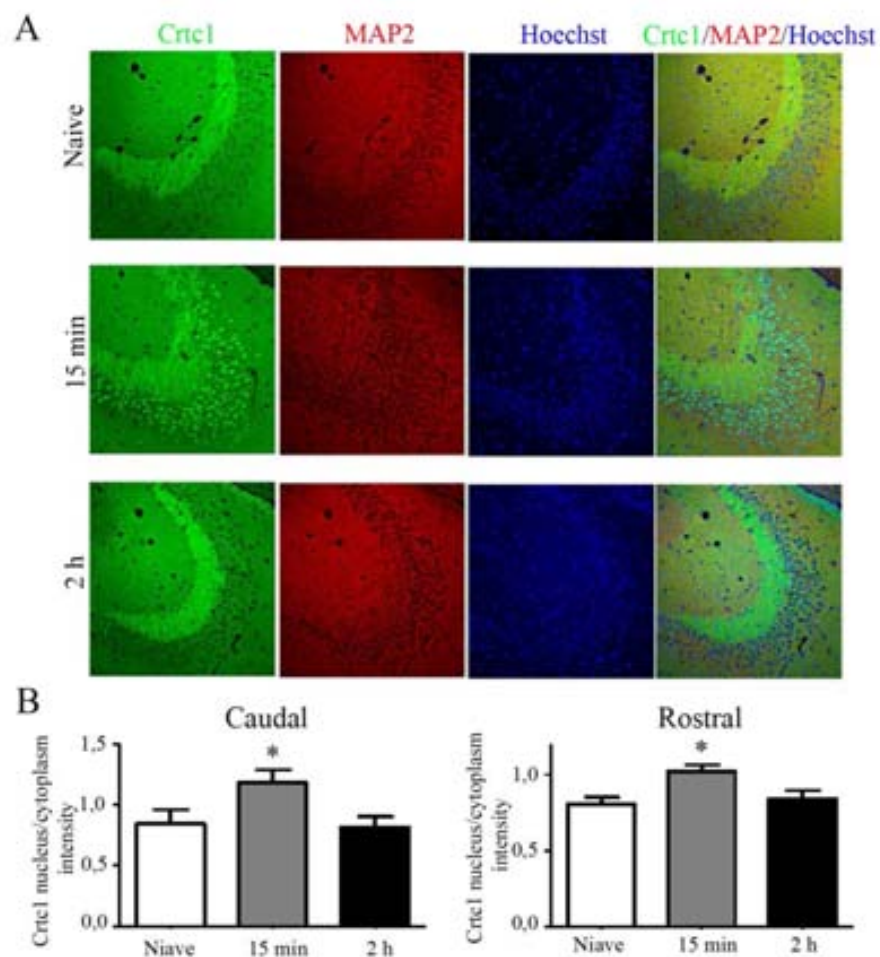


Figure 8 . Contextual learning induces nuclear translocation of Crtc1 in the hippocampus CA3.

A. Confocal microscopy images showing expression of Crtc1 (green), MAP2 (red) and Hoechst (blue) in CA3. Crtc1 translocated to nucleus 15 min after CFC training. **B.** Quantification of Crtc1 nucleus/cytoplasm intensity. * $P < 0.05$.

CA1 hippocampus, the area essential for rapid encoding of context representations during CFC (Anagnostaras et al., 2001). The mice were treated by 1) only handling (naïve), 2) 3 min's contextual exposure followed by shock plus 2 min's contextual exposure and sacrificed in 15 min after CFC (15 min) or 3) sacrificed in 2 h after CFC (2 h). Confocal imaging analysis revealed Crtc1

expressed in CA3 area and was abundantly present in the nucleus of CA3 pyramidal neurons 15 min but not 2 h after contextual fear conditioning compared to naïve mice (Fig. 8A). Quantitative imaging analysis revealed a rapid transient increase of Crtc1 in the nucleus of pyramidal neurons in CA3 caudal and rostral regions (Fig. 8B).

Crtc1 also expressed in CA1 area and moderately present in the nucleus after contextual fear conditioning compared to naïve mice (Fig. 9). Together, we conclude that Crtc1 is translocated from the cytosol and dendrites to the nucleus of hippocampal neurons after contextual learning.

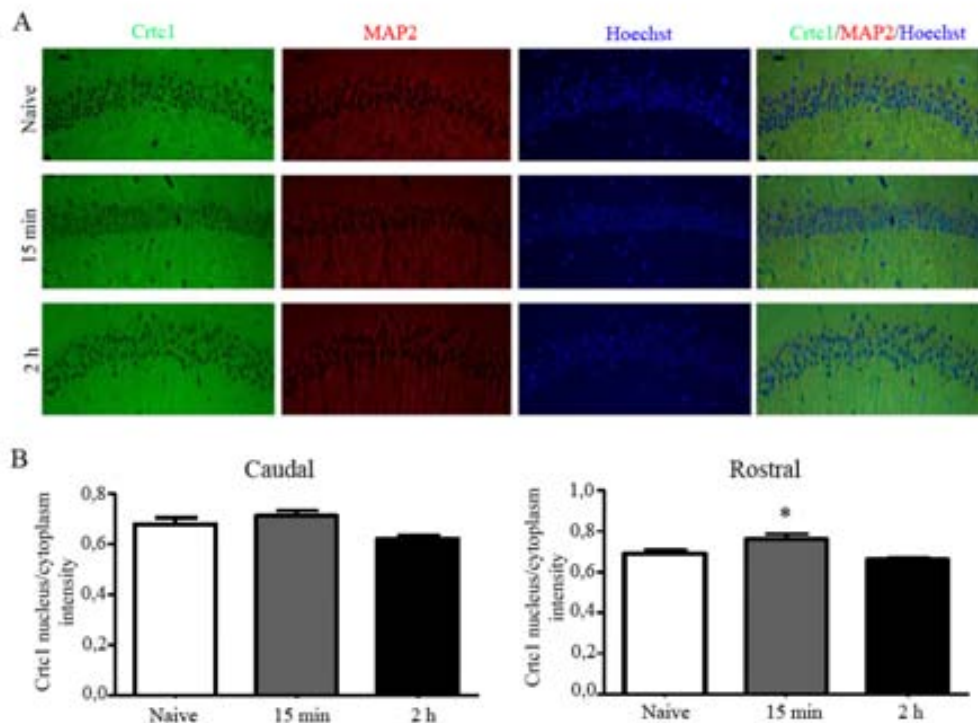


Figure 9 . Immunostaining images of Crtc1 labeling in the CA1 hippocampal neurons.

A. Confocal microscopy images showing expression of Crtc1 (green), MAP2 (red) and Hoechst (blue) in CA1. In contrast to CA3 region, only slight differences in Crtc1 nucleus translocation were observed in CA1 hippocampal region. **B.** Quantification of Crtc1 nucleus/cytoplasm intensity. * $P < 0.05$.

6.1.4 Contextual learning induces differential expression of C/EBP β /C/EBP δ -dependent genes

To explore the possibility that C/EBP β nuclear translocation could be mediating C/EBP-mediated transcription during associative learning, we examined the levels of CREB target genes in the above behavioral conditions (Fig. 5). We detected genes associated with neurotransmission and synaptic plasticity including *Arc*, *C-fos*, *Nr4a1-3*, *Bdnf IV*, *Nefl*, *Chga*, *Cyr61*, *Nrn1* and *Scg2a* (Parra-Damas et al., 2014). Gene expression was normalized to the geometric mean of *Gapdh*, hypoxanthine guanine phosphoribosyl transferase (*Hprt*) and peptidylprolyl isomerase A (*Ppia*) for brain samples. The stability of the reference genes was evaluated in each experiment using the NormFinder, BestKeeper and geNorm algorithms (Bustin et al., 2009). Contextual fear conditioning had a significant overall effect on hippocampal levels of *Arc* ($F(5,30) = 2.4, P = 0.05$), *c-fos* ($F(5,30) = 6.7, P = 0.0003$), *Nr4a1* ($F(5,30) = 3.5, P = 0.01$), *Nr4a2* ($F(5,30) = 2.8, P = 0.03$) (Fig. 10A), but not *Nr4a3*, *BDNF IV*, *Nefl*, *Chga*, *Cyr61*, *Nrn1* and *Scg2a* (Fig. 10B). *Arc* was similarly induced in the hippocampus by context or 15 min-24 h after fear conditioning but not by shock, which agrees with *Arc* activation by a novel context (Huff et al., 2006; Pevzner et al., 2012), (Fig. 10A). In contrast, *c-fos*, *Nr4a1* and *Nr4a2* levels were increased 15 min-24 h after fear conditioning but not by context or shock alone, while *Nr4a3* was not significantly changed (Figs. 10A, 10B). This result suggests activation of C/EBP β -dependent transcription in a differential manner by contextual learning in the dorsal hippocampus.

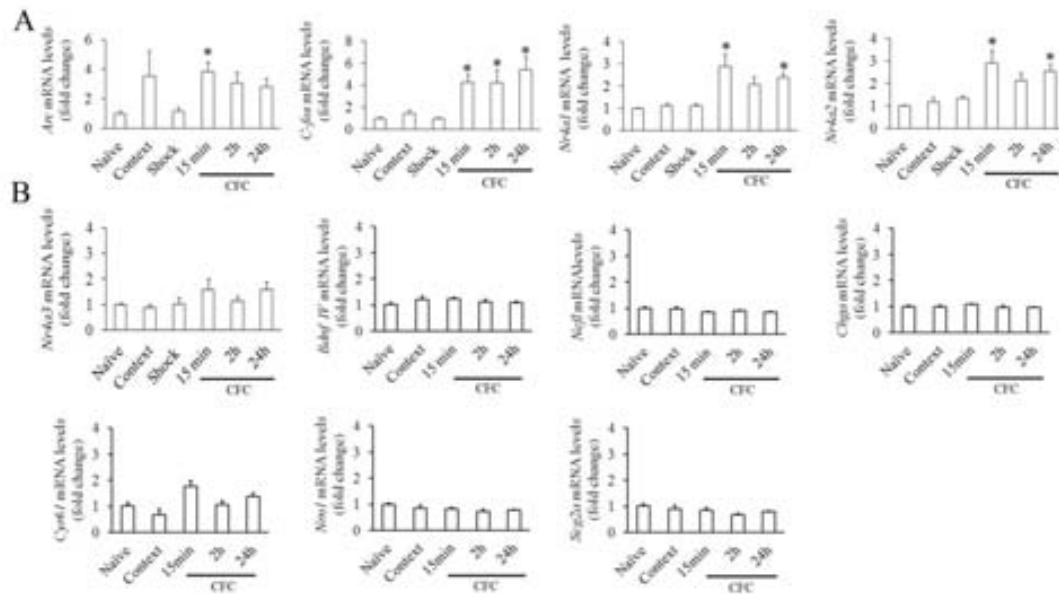


Figure 10. Quantitative analysis of mRNA transcripts in the hippocampus of contextual trained mice.

A, B, Levels of Arc, c-fos, Nr4a1, Nr4a2, Nr4a3, Bdnf, Nefl, Nrn1, Scg2a, Chga and Cyr61 transcripts were determined by real-time qRT-PCR and normalized to the geometric mean of standard genes GAPDH, Hprt1 and Ppia. Data represents mean \pm s.e.m (n=4-6 mice/group). *P < 0.05, ** P < 0.001, *** P < 0.0001, compared to naive mice as determined by one-way ANOVA followed by Bonferroni post hoc test.

6.1.5 Age-dependent contextual memory deficits in PS cDKO mice

The above results prompted us to investigate the contribution of *Crtc1* on contextual fear memory deficits in neurodegeneration. We studied presenilin (PS) conditional double knockout (cDKO) mice, an experimental model that develops age-dependent memory and synaptic plasticity deficits prior to cortical degeneration (Saura et al., 2004). At 2 months of age, control (WT) and PS cDKO mice displayed similar increased freezing responses 2 h and 24 h after CFC training (Fig. 11 left). Two-way ANOVA revealed significant main effect of training ($F(3,72) = 22.6, P = 0.0001$) but not genotype effect ($F(1,72) = 0.005,$

$P = 0.94$). These results indicate intact short-term and long-term contextual associative memories in PS cDKO mice at this age.

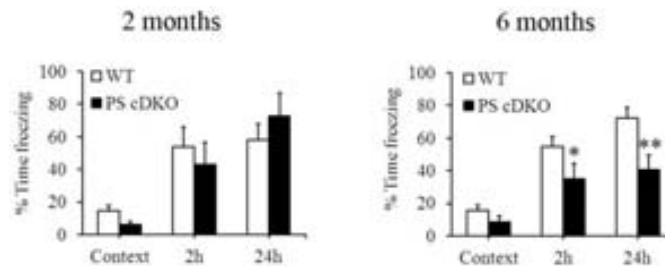


Figure 11. Age-dependent contextual memory deficits in PS cDKO mice

Left, Normal contextual memory in PS cDKO mice at 2 months. Different groups of control ($n=5-20$) and PS cDKO ($n=5-14$) mice were tested in one-shock contextual fear conditioning task. Freezing responses to the context before shock (neophobia) or immediately, 2 h and 24 h after shock were determined as a measure of immediate, short-term and long-term associative memories, respectively. Statistical significance is shown compared to freezing before shock. **Right**, Deficits in contextual memory in PS cDKO mice at 6 months. Different groups of control ($n=10-24$) and PS cDKO ($n=10-20$) mice were tested in one-shock contextual fear conditioning task as shown in Fig. 5A. PS cDKO mice show similar basal and immediate freezing responses than controls but significant decreased levels of freezing 2 h and 24 h after contextual training. $P < 0.05$, ** $P < 0.001$, *** $P < 0.0001$. Statistical analyses were performed by two-way ANOVA followed by Scheffé's S or Bonferroni post hoc test.

At 6 months of age, control mice displayed an increased freezing response 2h and 24h after training. By contrast, PS cDKO mice showed reduced freezing responses 2 h and 24 h after training compared to WT mice (Fig. 11 right). Two-way ANOVA revealed significant effects of training ($F(3,121) = 25$, $P = 0.0001$) and genotype ($F(1,121) = 21$, $P = 0.0001$). Post hoc analysis showed significant differences of freezing between control and PS cDKO mice at 2 h

and 24 h after training (Fig 5B). These results demonstrate age-dependent short- and long-term contextual memory deficits in PS cDKO mice.

6.1.6 Impairment of Crtc1 nuclear translocation in CA3 hippocampus in PS cDKO mice

We next investigated the relationship between Crtc1 nuclear translocation and function and contextual memory deficits in PS cDKO mice. Confocal imaging analyses showed that contextual learning induced rapid Crtc1 nuclear translocation as revealed by a significant increase of Crtc1 nucleus/cytoplasm ratio in CA3 pyramidal neurons of control mice ($P < 0.05$; **Fig. 12**). By contrast, Crtc1 was not efficiently translocated to the nucleus of pyramidal CA3 neurons in PS cDKO mice at the age of 4-5 months. (genotype effect: $F_{(1, 24)} = 4.03$, $P = 0.05$; **Fig. 12**). Together, these results suggested efficient Crtc1 nuclear translocation and transcription associated with contextual memory deficits in PS cDKO mice.

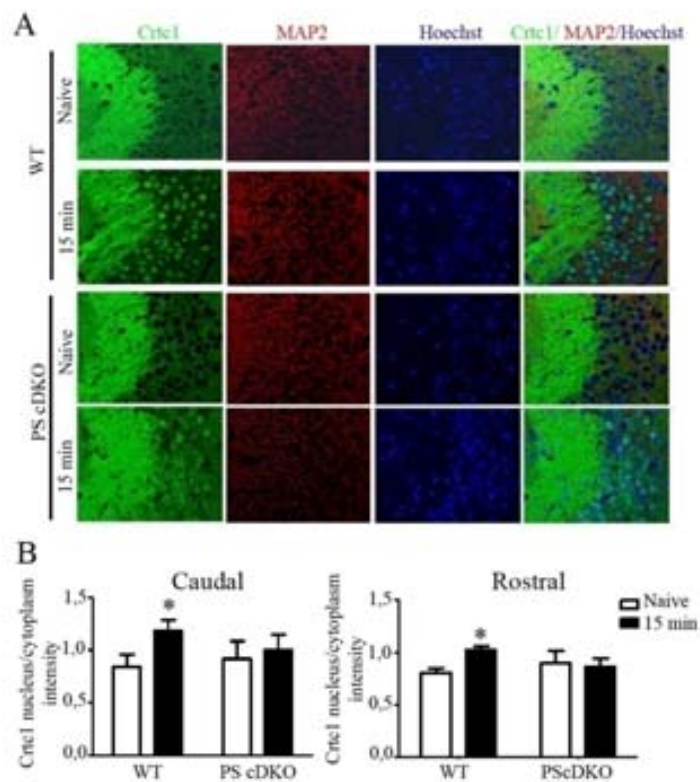


Figure 12. Impairment of Crtc1 nuclear translocation after CFC in CA3 hippocampus in PS cDKO mice.

A. Immunostaining images showed Crtc1 (green), MAP2 (red) and hoechst (blue) in CA3 in WT and PS cDKO mice 15 min after CFC training. Crtc1 translocated from cytoplasm to nucleus quickly after CFC training in WT mice, while PS cDKO mice showed the reduction of nuclear translocation after CFC training. **B.** Quantification of Crtc1 nucleus/cytoplasm ratio in WT and PS cDKO mice. * $P < 0,05$

6.1.7 Age-dependent Crtc1-dependent transcriptional deficits in PS cDKO mice

We next examined the induction of Crtc1/CREB-dependent genes after context or conditioning encoding in control and PS cDKO mice at 2 and

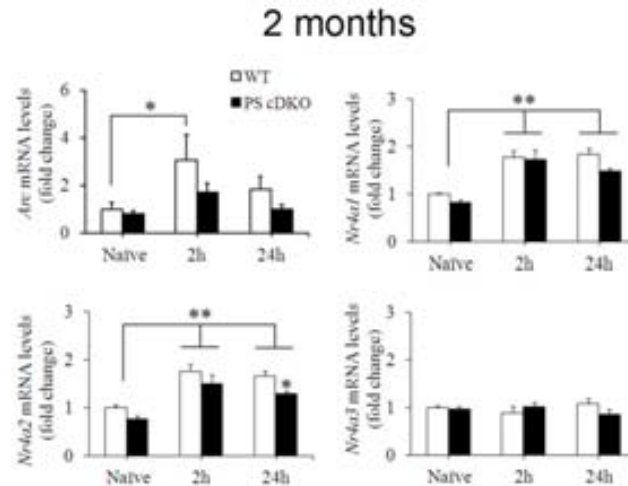


Fig.13 Levels of CRTC1-dependent gene transcripts in the hippocampus of control and PS cDKO mice at 2 months.

Levels of *Arc*, *Nr4a1*, *Nr4a2* and *Nr4a3* transcripts were determined by real-time qRT-PCR and normalized to the geometric mean of standard genes *GAPDH*, *Hprt1* and *Ppia*. Data represents mean \pm s.e.m (n=4-6 mice/group). *P < 0.05, ** P < 0.001, *** P < 0.0001. Statistical analyses were performed by two-way ANOVA followed by Scheffé's S or Bonferroni post hoc test.

6 months of age. *Arc* was significantly induced in the hippocampus of control mice after contextual training, whereas its expression was slightly reduced but not significantly changed in PS cDKO mice at 2 months (training effect: $F(2,22) = 3.4$, $P < 0.05$; genotype effect: $F(1,22) = 2.90$, $P = 0.10$; Fig. 13). *Nr4a1* and *Nr4a2* but not *Nr4a3* were significantly induced 2 h and 24 h after contextual learning in both genotypes (training effect, *Nr4a1*: $F(2, 22) = 23.7$, $P = 0.0001$; *Nr4a2*: $F(2, 22) = 19.3$, $P = 0.0001$; genotype effect, *Nr4a1*: $F(1, 22) = 3.60$, $P = 0.07$) except for *Nr4a2* ($F(1, 22) = 8.18$, $P = 0.01$). Post hoc analyses revealed non-significant differences between genotypes immediately, 2 h and 24 h after

training, except for *Nr4a2* at 24 h (Fig. 13; $P > 0.05$).

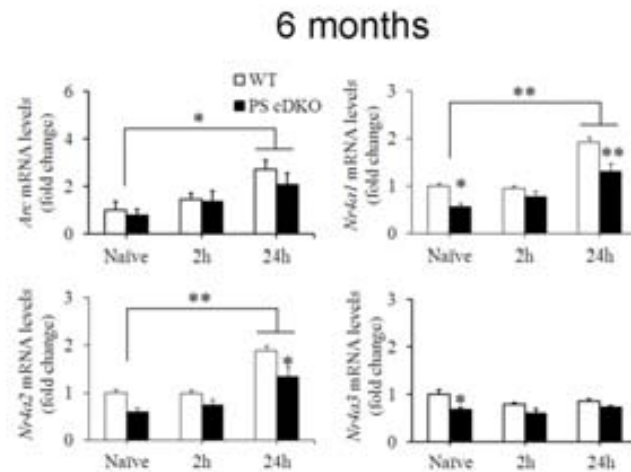


Figure 14 Levels of CRT C1-dependent gene transcripts in the hippocampus of control and PS cDKO mice at 6 months.

Levels of *Arc*, *Nr4a1*, *Nr4a2* and *Nr4a3* transcripts were normalized to the geometric mean of standard genes *GAPDH*, *Hprt1* and *Ppia*. Data represents mean \pm s.e.m ($n=4-6$ mice/group). * $P < 0.05$, ** $P < 0.001$, *** $P < 0.0001$. Statistical analyses were performed by two-way ANOVA followed by Scheffé's S or Bonferroni post hoc test.

At 6 months of age, *Arc* was significantly increased 24 h after contextual training but without significant differences between genotypes (training effect: $F(2, 29) = 6.9$, $P = 0.005$; genotype effect: $F(1, 29) = 0.85$, $P = 0.36$) (Fig. 14). In basal conditions, *Nr4a1*, *Nr4a2* and *Nr4a3* were slightly reduced in PS cDKO mice, whereas *Nr4a1* and *Nr4a2*, but not *Nr4a3*, were differentially increased 24 h after contextual learning in control and PS cDKO mice (training effect, *Nr4a1*: $F(2, 29) = 33.0$, $P = 0.0001$; *Nr4a2*: $F(2, 29) = 27.9$, $P = 0.0001$; genotype effect, *Nr4a1*: $F(1, 29) = 18.1$, $P = 0.0002$; *Nr4a2*: $F(1, 29) = 14.8$, $P = 0.0006$).

(Fig. 14). Post hoc analysis revealed a significant reduction of *Nr4a1* ($P < 0.001$) and *Nr4a2* ($P < 0.01$) but not *Nr4a3* ($P > 0.05$) in the hippocampus of PS cDKO at 24 h. These results indicated a gene-related hippocampal *Crtc1*-dependent transcriptional deficits associated with contextual memory impairments in PS cDKO mice.

6.1.8 *Crtc1* gene transfer reverses *Crtc1*-dependent transcription changes and associative memory deficits in PS cDKO mice

To assess whether *Crtc1* dysfunction contributed to associative memory deficits in PS cDKO mice, we expressed exogenous mouse *Crtc1* *in vivo* with a recombinant adeno-associated virus (AAV2/10) characterized by high gene transduction in neurons (Klein et al., 2008; Parra-Damas et al., 2014). We injected AAV-*Crtc1*-myc or -GFP (control) in CA3 hippocampus of control and PS cDKO mice at 4 months of age. For viral injections, 4-5 month-old mice ($n=8$ mice/group) were anesthetized with isoflurane and placed in a stereotaxic platform (Kopf, Tujunga, CA, USA). The stereotaxic injection coordinates for the hippocampus were (in mm) as follows: anterior 0.2 caudal to Bregma; 0.18 lateral to Bregma; depth 0.2 ventral to dural surface according to (Paxinos and Franklin, 2004). AAV vector stocks (3×10^{11} gc/ml; $0.5 \mu\text{l}/\text{min}$) were injected bilaterally into the hippocampus through a 27 gauge cannula connected to a $10 \mu\text{l}$ Hamilton syringe. Four weeks after AAV injection mice were handled, behavioral tested, sacrificed and dissected.

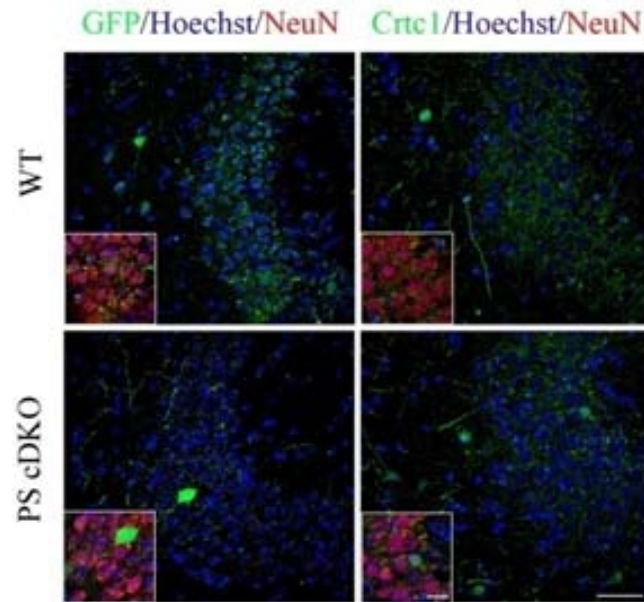


Figure 15. Long-term expression of CRTC1-myc in mouse CA3.

CRTC1-myc (green) was efficiently expressed in neurons at the injection point, CA3 regions of the hippocampus three weeks after intrahippocampal injection with AAV2/10-CRTC1-myc vectors. NeuN (red), Hoechst (blue): nucleus. Scale bar: 30 μ m.

Mice coronal sections were stained for exogenous Crtc1, NeuN and nucleus. AAV-Crtc1 injection resulted in long-term and wide expression of Crtc1-myc in CA3 neurons (Fig. 15). In addition, RTPCR analysis showed that AAV-Crtc1 injection leads to Crtc1-myc mRNA expression in hippocampus (Fig. 16 bottom). Moreover, biochemical analysis detected the Crtc1-myc expression in hippocampus (Fig. 16 top).

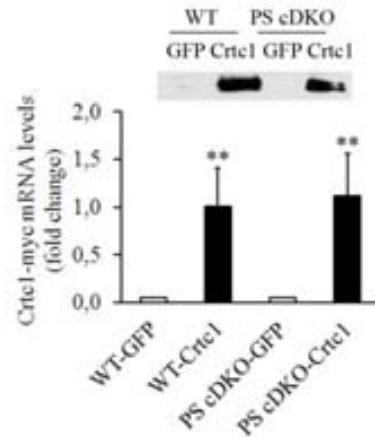


Figure 16. Long-term expression of CRTC1-myc in mouse hippocampus.

Increased exogenous Crtc1-myc (top) and total Crtc1 (bottom) mRNAs normalized to Gapdh in WT and PS cDKO mice injected with AAV2/10-CRTC1. Data are the mean \pm s.e.m (n=4-5 mice/group). * $P < 0.05$, ** $P < 0.001$, compared to AAV2/10-GFP-injected control mice. Statistical analysis was performed by one-way ANOVA.

When evaluated in contextual fear conditioning, WT AAV-GFP mice displayed an increased freezing response 24h after training, while PS cDKO AAV-GFP mice showed a reduced freezing response 24h after training. We found significant effects of group ($F(3,42) = 4.3, P = 0.01$), training time ($F(1,42) = 36.8, P = 0.0001$) and group x training time interaction ($F(3,42) = 3.5, P = 0.02$, two-way ANOVA) (Fig. 17A). AAV-Crtc1 increased significantly freezing responses 24h after training both in WT ($P = 0.05$) and PS cDKO mice ($P = 0.03$) compared to GFP-injected groups (Fig. 17A).

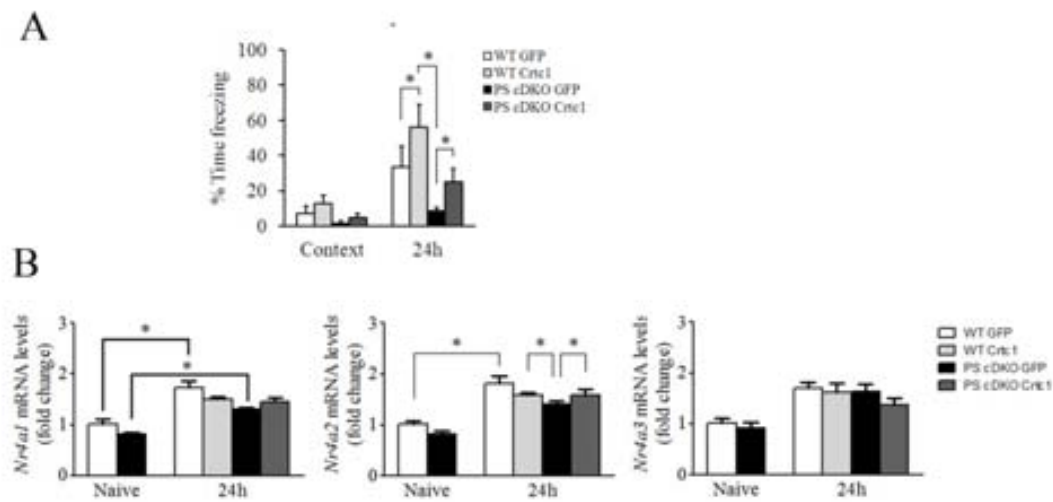


Figure 17. Injection of AAV-CRTC1 rescues deficits of associative memory and Crtc1-dependent gene expression deficits in 6 month-old PS cDKO mice three weeks after expression.

A. Data are the mean \pm s.e.m (n=8 mice/group). *P < 0.005, ** P < 0.001. Statistical analyses determined by two-way ANOVA and Scheffé's S post hoc test. **B.** Data represents the mean \pm s.e.m (n=4-5 mice/group). mRNA levels are normalized to the geometric mean of *Gad6h*, *Hprt1* and *Tbp*. *P < 0.05. Statistical analyses were determined by two-way ANOVA followed by Student-Newman-Keuls post hoc test.

We next examined mRNA levels of Crtc1-dependent genes in the above experimental groups. WT AAV-GFP mice display an increased *Nr4a1* and *Nr4a2* gene expression 24h after CFC training in the hippocampus, while PS cDKO AAV-GFP mice showed a reduced *Nr4a1* and *Nr4a2* gene expression levels. Importantly, Crtc1 injection increased significantly *Nr4a1* and *Nr4a2* but not *Nr4a3* in the hippocampus of trained PS cDKO mice compared to GFP-injected controls (Fig. 17B). These results demonstrated that increasing Crtc1 function ameliorates hippocampal-dependent long-term contextual memory deficits by

enhancing a specific subset of CREB target genes.

6.1.9 Effect of *Crtc1* on brain degeneration in *PS cDKO* mice

PS cDKO mice display an age-dependent neurodegeneration. Previous studies detected progressive and striking loss of cerebral cortical gray and white matter accompanied by enlargement of the lateral ventricles in *PS cDKO* mice. *PS cDKO* mice at 6-9 months of age showed a reduction in neuronal number and neocortical volume compared to WT mice (Saura CA, et al., 2004).

PS cDKO mice develop dendritic degeneration and cortical neuron loss during aging (Fig. 18) (Saura et al., 2004). In agreement with the previous studies, Nissl staining showed that *PS cDKO* mice injected with GFP at 6 months of age display an apparent thinning of the cerebral cortex compared to WT mice (Fig. 18). A AV-mediated *Crtc1* injection in the hippocampus of *PS cDKO* mice did not affect apparently cortical layering and thickness and enlargement of lateral ventricles in *PS cDKO* mice at 6 months (Fig. 18). Quantitative measures of cortical thickness of multiple mice ($n = X$ /group) revealed 27% decrease of thickness of *PS cDKO*-GFP mice compared to WT-GFP mice. Cortical thickness of *PS cDKO*-*Crtc1* mice did differ significantly from *PS cDKO*-GFP mice (Fig. 18).

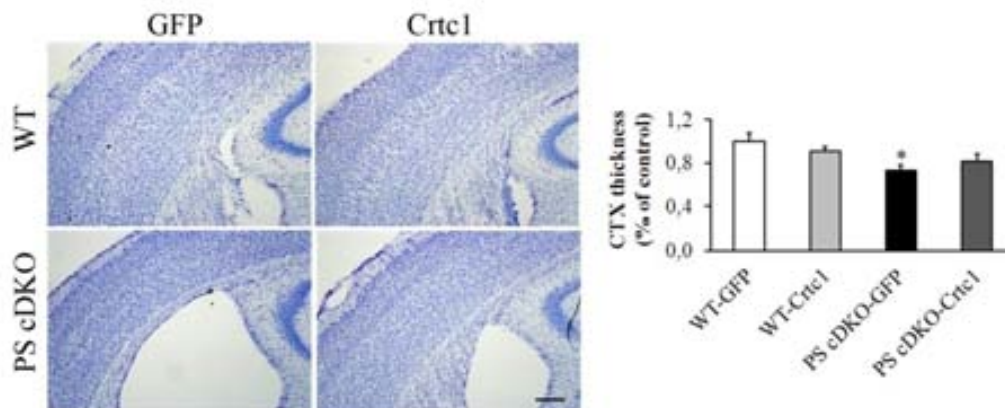


Figure 18. Neurodegeneration in PS cDKO mice.

A. Nissl staining of thickness in cortex. Nissl-stained images of coronal sections in cortex from WT and PS cDKO mice injected with AAV-GFP or -Crtc1 are shown. Scale bar: 200 μ m. **B.** Quantification of thickness in cortex. * $P < 0.05$.

In addition, Nissl staining did not reveal apparent gross differences in CA1, CA3 and DG areas of the hippocampus in PS cDKO mice injected with AAV-GFP or -Crtc1 at 6 months of age (Fig. 19).

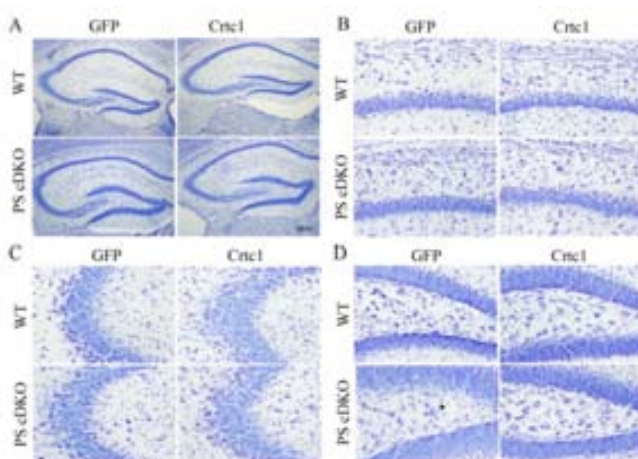


Figure 19. Nissl staining in Hippocampus.

Nissl-stained images of coronal sections in hippocampus, CA1, CA3 and DG from WT and PS cDKO mice injected with AAV-GFP or -Crtc1 are shown. Scale bar: 200 μ m.

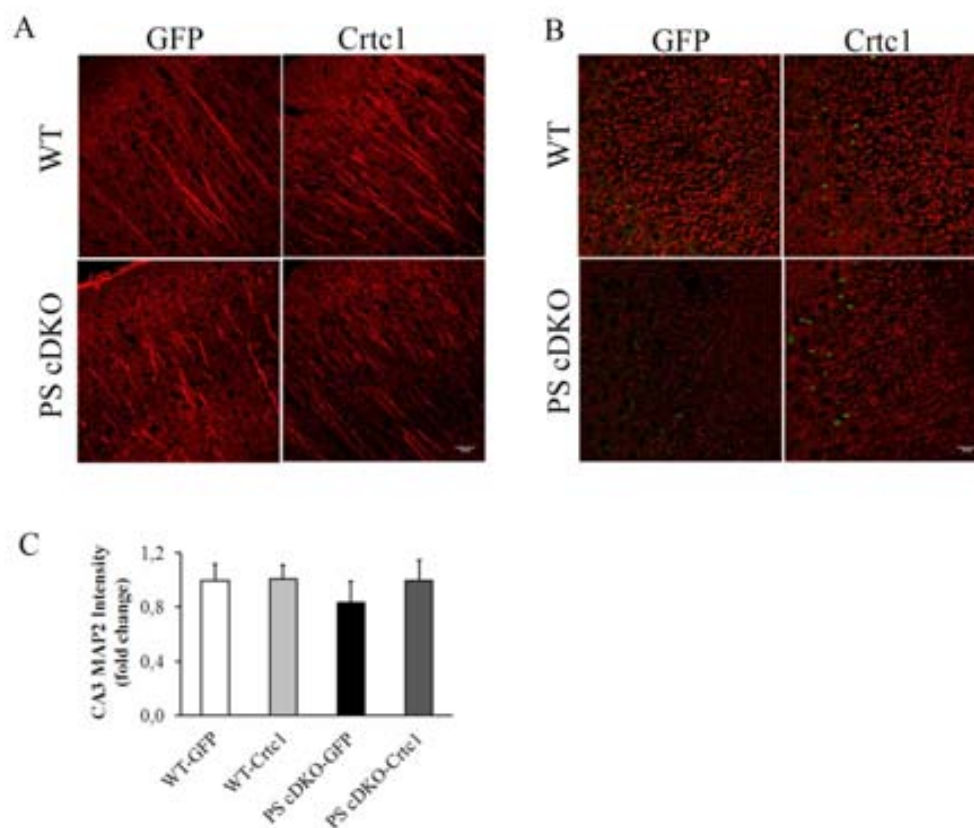


Figure 20. Effect of Crtc1 on dendritic degeneration in PS cDKO mice

A. MAP2 staining images of coronal sections in cortex from WT and PS cDKO mice injected with AAV-GFP or -Crtc1. Scale bar: 20 μ m. **B.** MAP2 staining images of coronal sections in hippocampus from WT and PS cDKO mice injected with AAV-GFP or -Crtc1. Scale bar: 20 μ m. **C.** Quantification of MAP2 intensity in CA3 hippocampus.

We next examined dendritic morphology by applying immunofluorescence staining, a more sensitive method, with MAP2 antibody to analyze possible changes on dendrites. MAP2 staining (in red) showed apparent reduced number and length of dendrites in the neocortex in 6 month-old GFP-injected PS cDKO mice (Fig. 20). AAV-Crtc1 injection in the hippocampus did not affect dendritic morphology in WT or PS cDKO mice (Fig. 20). Similarly, 6

month-old PS cDKO-GFP mice display an apparent decrease of MAP2 staining in CA3 hippocampus compared to WT-GFP mice. Crtc1 overexpression (in green) enhanced MAP2 staining in PS cDKO mice although quantification of total MAP2 staining did not reveal significant differences due to high experimental variability (Fig 20).

6.1.10 CRTC1 protein changes in human brain at AD pathological stages

To investigate changes in CRTC1 protein changes during the progression of AD pathology, we analyzed the hippocampus of 42 individuals pathologically classified as controls (no pathology, n= 12), early (Braak I–II, n=12), intermediate (Braak III–IV, n= 10), and advanced (Braak V–VI, n= 8) pathological stages (Braak et al., 2006). Brain samples were closely matched for age, neurofibrillary pathology, postmortem delay and RIN values (see methods). Biochemical analysis revealed a reduction of both total and phosphorylated CRTC1 in human hippocampus at Braak IV and V–VI pathological stages (Fig. 21). These results indicated decreased CRTC1 levels in human brain at intermediate Braak III–VI pathological stages.

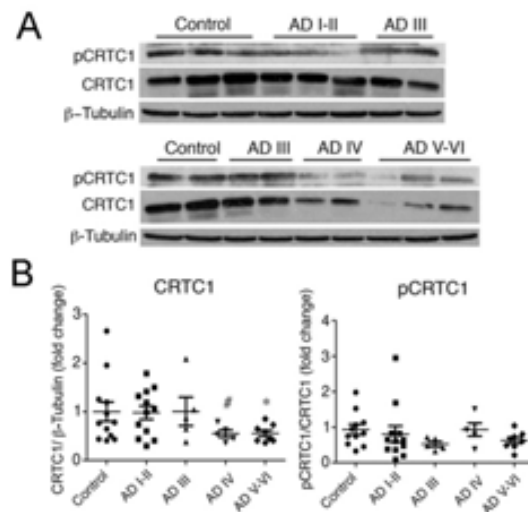


Fig. 21 CRTC1 protein changes in human brain at AD pathological stages

A. Western blotting of total and phosphorylated (Ser151) CRTC1 (pCRTC1) in human hippocampus at different AD stages. Values represent mean fold change \pm SEM (n=5–12 per group). **B.** Quantification of WB. * $p < 0.05$ compared with control as determined by one-way ANOVA followed by Scheffe's S post hoc test.

Discussion

Discussion

CREB facilitates short- and long-term contextual memories by enhancing neuronal excitability and recruitment of neurons into memory networks (Won and Silva, 2008; Restivo et al., 2009; Viosca et al., 2009; Suzuki et al., 2011). Besides efforts to identify the CREB transcriptome (Cha-Molstad et al., 2004; Zhang et al., 2005), the CREB transcriptional programs that selectively mediate associative memory are still unclear. We found that contextual learning induces Crtc1 dephosphorylation and nuclear translocation leading to activation of a CREB gene program in the hippocampus mediating associative memory encoding. Importantly, Crtc1 can be critical for long-term associative memory since Crtc1 nuclear translocation and transcription deficits are associated with contextual memory impairments in *PS* mutant mice. These results indicate for the first time a role of Crtc-dependent transcription in associative memory in normal and pathological conditions.

A relevant finding of our study is that associative learning activates Crtc1-dependent transcription in the hippocampus. Crtc1 activation involves translocation of Crtc1 from the cytosol and dendrites to the nucleus of hippocampal neurons, a mechanism important for activity-dependent Crtc1 activation in cultured neurons (Zhou et al., 2006; Ch'ng et al., 2012). Interestingly, contextual learning but not novel context or shock selectively induces time-dependent Crtc1 nuclear translocation in fear memory regions. Crtc1 translocation is regulated in a time and region specific manner, being predominant in CA3 hippocampus and to a minor extent in CA1 hippocampus and basolateral amygdalar neurons. In agreement, contextual learning, but not contextual alone or shock, induces expression of CREB target genes dependent on Crtc1, including *Nr4a1* and *Nr4a2* but not *Nr4a3* (España et al., 2010b; Breuillaud et al., 2012) (Fig. 4). This result agrees with previous findings indicating induction of *Nr4a* nuclear receptors subfamily genes in the hippocampus by contextual learning, whereas blocking NR4A function impairs contextual memory (Rojas et al., 2007; Hawk et al., 2012). By contrast, *Arc* is similarly induced by context and immediately, shortly and long-term after contextual learning, indicating that *Arc* is not specifically induced by associative learning. Whereas context exploration is known to induce *Arc* in the hippocampus (Huff et al., 2006; Pevzner et al., 2012), our results do not preclude the possibility that *Arc* or other immediate early genes could be up-regulated by associative learning in the prefrontal cortex (Tse et al., 2011). These results also agree with activation of CREB-mediated transcription by contextual learning in CA1/CA3 hippocampus, which contrasts with CREB activation by cued fear-conditioning in the amygdala (Impey et al.,

1998). In conclusion, contextual learning activates *Crtc1* specifically in the dorsal hippocampus, a region genetically activated by contextual learning that is required for encoding of contextual memory (Lee and Kesner, 2004; Ramamoorthi et al., 2011).

Long-lasting synaptic plasticity and contextual learning activate CREB-mediated transcription by increasing CREB phosphorylation at Ser133 (Impey et al., 1996; Impey et al., 1998; Kudo et al., 2004), a mechanism that is essential but not sufficient for gene transcription (Chrivia et al., 1993; Bito et al., 1996). Notably, CREB phosphorylation is similarly induced by novel context and after fear conditioning indicating that this process is independent of context-cued association. By contrast, context learning, but not context alone or shock, induces *Crtc1* dephosphorylation at Ser151, a process critical for activity-induced CREB-mediated transcription (Altarejos et al., 2008; España et al., 2010b). Phosphorylation at Ser151, a site homologous to *Crtc2* Ser171 or *Crtc3* Ser162, mediates *Crtc* binding to 14-3-3 protein and sequestration into the cytoplasm (Screaton et al., 2004; Clark et al., 2012). Although several phosphorylation sites in *Crtc* may regulate CREB-dependent transcription and nuclear import (Ch'ng et al., 2012), our results point to a direct role of Ser151 on gene transcription during contextual memory. We cannot discard the possibility that *Crtc1* transcriptional function could be regulated by alternative mechanisms in neurons including kinase/phosphatase activities, synapse-nuclear translocation, acetylation or CREB glycosylation (España et al., 2010b; Ch'ng et al., 2012; Jeong et al., 2012; Rexach et al., 2012).

Genetic and biochemical evidences suggest a role of CREB in cognitive and neurodegenerative disorders (Saura and Valero, 2011). However, the age-related *Crtc1*-dependent transcriptional and nuclear translocation deficits observed in *PS* cDKO mice is the first evidence linking *Crtc1* dysfunction and associative memory impairments in neurodegeneration. Memory deficits in *PS* cDKO mice were previously associated with CREB-dependent gene changes and CBP dysfunction (Saura et al., 2004). Indeed, CBP-deficient mice show short- and long-term memory deficits in fear conditioning paradigms likely caused by failure of CREB-dependent gene expression (Bourtchouladze et al., 2003; Alarcon et al., 2004; Chen et al., 2010; Barrett et al., 2011). Moreover, *Crtc1* transcriptional deficits were recently associated with early spatial memory impairments in AD transgenic mice (Parra-Damas et al., 2014), whereas reduced CBP/CREB target genes are linked to cognitive deficits in Huntington's disease mutant mice (Giralt et al., 2012).

Does *Crtc1*-dependent transcription contribute to associative memory deficits during neurodegeneration? To address this question we performed *Crtc1* gene therapy *in vivo* and demonstrated that enhancing *Crtc1* expression and transcriptional function ameliorated long-term contextual memory deficits in *PS* cDKO mice. These results together with the fact that *Crtc1* expression before training facilitates fear memory consolidation (Sekeris et al., 2012) reinforce the view for a direct role of *Crtc1* on associative memory impairments. Interestingly, *Crtc1* overexpression reversed dendrite morphology changes in the hippocampus of *PS* cKO mice suggesting that morphological and memory changes are linked. Indeed, *Crtc1* regulates BDNF-mediated dendritic growth in cortical neurons (Finsterwald et al., 2010). Similarly to CREB enhancement (Gong et al., 2004; Caccamo et al., 2011; Yiu et al., 2011), *Crtc1* gene transfer ameliorates early hippocampal-dependent spatial memory deficits in AD transgenic mice (Parra-Damas et al., 2014). Since dementia patients develop deficits in associative memory encoding and retrieval (Granholm and Butters, 1988; Hamann et al., 2002; Hoefer et al., 2008), these results are relevant for future therapeutics in AD and cognitive-related disorders. Targeting *Crtc1* and increasing selectively expression of genes mediating contextual learning could be a promising avenue to ameliorate associative memory deficits in cognitive disorders.

Hypothesis & Conclusions

Hypothesis

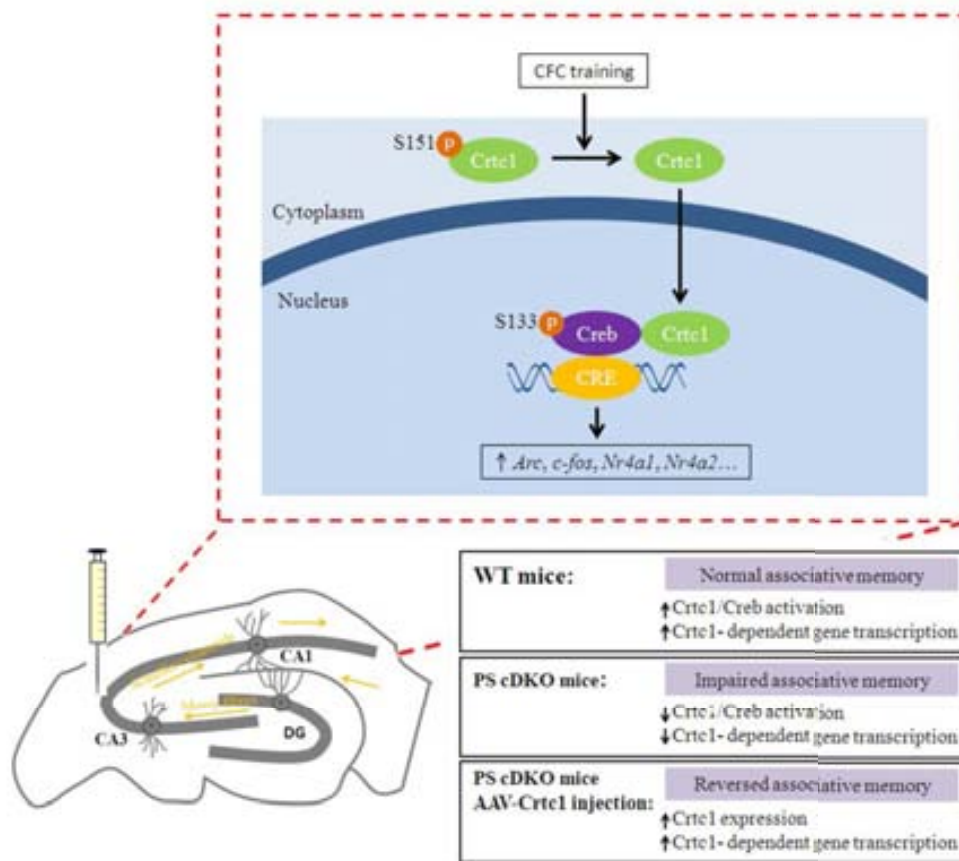


Figure 1. Role of Crtc1 in contextual fear memory

The results of this doctoral thesis strongly suggest a role of Crtc1 in contextual fear memory (Figure 1). Contextual fear conditioning training induces Crtc1 dephosphorylation at ser151 and nuclear translocation in the hippocampus of mice. Nuclear Crtc1 interacts with activated Creb to increase expression of Crtc1/Creb dependent genes related to neurotransmission and synaptic plasticity such as *Arc*, *c-fos*, *Nr4a1* and *Nr4a2*. By contrast, PS cDKO mice display a gene-dependent impairment of contextual fear memory associated to a decrease of Crtc1 translocation and Crtc1-dependent gene transcription. Importantly, overexpression of Crtc1 in the CA3 hippocampus reverses the impairment of associative memory and Crtc1-dependent gene transcription in PS cDKO mice.

Conclusions

1. The transcription factor Creb and its coactivator Crtc1 are activated upon synaptic stimulation in neurons
2. Contextual fear conditioning training activates Creb and Crtc1 in the hippocampus but not in the cortex
3. Contextual fear conditioning induces Crtc1-dependent gene expression in the hippocampus
4. *PS* cDKO mice display age-dependent associative memory deficits, neurodegeneration and Crtc1-dependent transcriptional changes
5. Crtc1 gene transfer rescues contextual associative memory deficits and Crtc1-dependent transcription in *PS* cDKO mice
6. CRT1C1 levels are reduced in human hippocampus at intermediate Braak III/IV pathological stages

Reference

Reference

1. Alberini C M (2009) T ranscription f actors i n l ong-term me mory a nd synaptic plasticity. *Physiological reviews* 89:121.
2. Altarejos JY, Goebel N, Conkright MD, Inoue H, Xie J, Arias CM, Sawchenko PE, Montminy M (2008) The CREB1 coactivator CRTC1 is required for energy balance and fertility. *Nat Med.* 14:1112-7.
3. Altarejos JY and Montminy M (2011) CREB and the CRTC co-activators: sensors for hormonal and metabolic signals. *Nat Rev Mol Cell Biol.* 12:141-51.
4. Amelio AL, Caputi M, Conkright MD (2009) Bipartite functions of the CREB co-activators selectively direct alternative splicing or transcriptional activation. *EMBO J.* 28:2733-47.
5. Anagnostaras SG, Gale GD, Fanselow MS (2001) Hippocampus and contextual fear conditioning: recent controversies and advances. *Hippocampus.* 11:8-17.
6. Bach ME, Barad M, Song H, Zhuo M, Lu YF, Shih R, Mansuy I, Hawkins RD, Kandel ER (1999) Age-related defects in spatial memory are correlated with defects in the late phase of hippocampal long-term potentiation in vitro and are attenuated by drugs that enhance the cAMP signaling pathway. *Proc Natl Acad Sci U S A.* 96:5280-5.
7. Ballard C, Gauthier S, Corbett A, Brayne C, Arslan D, Jones E (2011) Alzheimer's disease. *Lancet.* Mar 377:1019-31.
8. Ballatore C, Lee VMY, Trojanowski JQ (2007) Tau-mediated neurodegeneration in Alzheimer's disease and related disorders. *Nature Reviews Neuroscience.* 8:663–672.
9. Barad M, Bourtchouladze R, Winder DG, Golan H, Kandel E (1998) Rolipram, a type IV-specific phosphodiesterase inhibitor, facilitates the establishment of long-lasting long-term potentiation and improves memory. *Proc Natl Acad Sci U S A.* 95:15020-5.
10. Bitto H, Deisseroth K, and Tsien RW (1996). CREB phosphorylation and dephosphorylation: a Ca^{2+} - and stimulus duration-dependent switch for hippocampal gene expression. *Cell* 87, 1203 – 1214.

11. Bittinger MA, McWhinnie E, Meltzer J, Iourgenko V, Latario B, Liu X, Chen CH, Song C, Garza D, Labow M (2004) Activation of cAMP response element-mediated gene expression by regulated nuclear transport of TORC proteins. *Curr Biol.* 14:2156-61.
12. Bourtchuladze R, Frenguelli B, Blendy J, Cioffi D, Schutz G, and Silva AJ (1994). Deficient long-term memory in mice with a targeted mutation of the c-AMP-responsive element binding protein. *Cell* 79, 59 – 68.
13. Braak H, Braak E (1991) Demonstration of amyloid deposits and neurofibrillary changes in whole brain sections. *Brain Pathol.* 1:213-6.
14. Braak H, Alafuzoff I, Arzberger T, Kretschmar H, Del Tredici K (2006) Staging of Alzheimer disease-associated neurofibrillary pathology using paraffin sections and immunocytochemistry. *Acta Neuropathol.* 112:389-404.
15. Brunden KR, Trojanowski JQ, Lee VM (2009) Advances in Tau-focused drug discovery for Alzheimer's disease and related tauopathies *Nat Rev Drug Discov.* 8: 783–793.
16. Bustin SA, Benes V, Garson JA, Hellemans J, Huggett J, Kubista M, Mueller R, Nolan T, Pfaffl MW, Shipley GL, Vandesompele J, Wittwer CT (2009) The MIQE guidelines: minimum information for publication of quantitative real-time PCR experiments. *Clin Chem.* 55:611-22.
17. Ch'ng TH, Uzgil B, Lin P, Avliyakov N K, O'Dell T J, Martin K C (2012) Activity-dependent transport of the transcriptional coactivator CTCF from synapse to nucleus. *Cell.* 150:207-21.
18. Chowdhury S, Shepherd JD, Okuno H, Lyford G, Petralia RS, Plath N, Kuhl D, Huganir RL, Worley PF (2006) Arc/Arg3.1 interacts with the endocytic machinery to regulate AMPA receptor trafficking. *Neuron* 52:445-459
19. Cohen S, Greenberg ME (2008) Communication between the synapse and the nucleus in neuronal development, plasticity, and disease. *Annu Rev Cell Dev Biol.* 24:183-209.
20. Comb, M., Birnberg, N. C., Seasholtz, A., Herbert, E. & Goodman, H. M (1986) A cyclic AMP- and phorbol ester-inducible DNA element. *Nature* 323, 353–356.
21. Conkright MD, Canettieri G, Sreton R, Guzman E, Miraglia L, Hogenesch JB,

- Montminy M (2003) TORCs: transducers of regulated CREB activity. *Mol Cell.* Aug;12:413-23.
22. Corder EH, Saunders AM, Sittmayer WJ, Schmechel DE, Gaskell PC, Small GW, Roses AD, Haines JL, Pericak-Vance MA (1993) Gene dose of apolipoprotein E type 4 allele and the risk of Alzheimer's disease in late onset families. *Science.* 261:921-3.
23. De Strooper B, Saftig P, Craessaerts K, Vanderstichele H, Guhde G, Annaert W, Von Figura K, Van Leuven F (1998) Deficiency of presenilin-1 inhibits the normal cleavage of amyloid precursor protein. *Nature.* 391:387-90.
24. Dermaut B, Kumar-Singh S, Engelborghs S, Theuns J, Rademakers R, Saerens J, Pickut BA, Peeters K, van den Broeck M, Vennekens K, Claes S, Cruts M, Cras P, Martin JJ, Van Broeckhoven C, De Deyn PP (2004) A novel presenilin 1 mutation associated with Pick's disease but not beta-amyloid plaques. *Ann Neurol.* 55:617-26.
25. Deisseroth K, Tsien RW (2002) Dynamic multiphosphorylation pathways for activity-dependent gene expression. *Neuron.* 34:179-82.
26. DeZazzo J, Tully T. Dissection of memory formation: from behavioral pharmacology to molecular genetics (1995) *Trends Neurosci.* 18:212-8.
27. Dickey CA, Loring JF, Montgomery J, Gordon MN, Eastman PS, Morgan D (2003) Selectively reduced expression of synaptic plasticity-related genes in amyloid precursor protein + presenilin-1 transgenic mice. *J Neurosci.* 23:5219-26.
28. Donoviel DB, Hadjantonakis AK, Ikeda M, Zheng H, Hyslop PS, Bernstein A. (1999) Mice lacking both presenilin genes exhibit early embryonic patterning defects. *Genes Dev.* 13, 2801–2810
29. Dynlacht BD (1997) Regulation of transcription by proteins that control the cell cycle. *Nature.* 389:149-52.
30. Ferrer I, Marín C, Rey MJ, Ribalta T, Goutan E, Blanco R, Tolosa E, Martí E (1999) BDNF and full-length and truncated TrkB expression in Alzheimer disease. Implications in therapeutic strategies. *J Neuropathol Exp Neurol.* 58:729-39.
31. Fleischmann A, Hvalby O, Jensen V, Strekalova T, Zacher C, Layer LE, Kvello A, Reschke M, Spanagel R, Sprengel R, Wagner EF, Gass P (2003) Impaired long-

- term memory and NR2A-type NMDA receptor-dependent synaptic plasticity in mice lacking c-Fos in the CNS. *J Neurosci.* 23:9116-22.
32. Fortini ME (2002) Gamma-secretase-mediated proteolysis in cell-surface-receptor signalling. *Nat Rev Mol Cell Biol.* 3:673-84.
33. Gauthier S, Vellas B, Farlow M, Burn D (2006) Aggressive course of disease in dementia. *Alzheimers Dement.* 2:210-7.
34. Glenner GG, Wong CW (1984) Alzheimer's disease: initial report of the purification and characterization of a novel cerebrovascular amyloid protein. *Biochem Biophys Res Commun.* 120:885-890.
35. Gong B, Vitolo OV, Trinchese F, Liu S, Shelanski M, Arancio O (2004) Persistent improvement in synaptic and cognitive functions in an Alzheimer mouse model after rolipram treatment. *J Clin Invest.* 114:1624-34.
36. Gonzalez GA, Montminy MR (1989) Cyclic AMP stimulates somatostatin gene transcription by phosphorylation of CREB at serine 133. *Cell.* 59:675-80.
37. Graham R, Gilman M (1991) Distinct protein targets for signals acting at the c-fos serum response element. *Science* 251:189.
38. Granholm E, Butters N (1988) Associative encoding and retrieval in Alzheimer's and Huntington's disease. *Brain Cogn.* 7:335-47.
39. Greer PL, Greenberg ME (2008) From synapse to nucleus: calcium-dependent gene transcription in the control of synapse development and function. *Neuron* 59:846-860.
40. Guzowski JF, Lyford GL, Stevenson GD, Houston FP, McLaugh JL, Worley PF, Barnes CA (2000). Inhibition of activity-dependent Arc protein expression in the rat hippocampus impairs maintenance of long-term potentiation and the consolidation of long-term memory. *J Neurosci.* 20:3993-4001.
41. Guzowski JF, Setlow B, Wagner EK, McLaugh JL (2001). Experience-dependent gene expression in the rat hippocampus after spatial learning: a comparison of immediate-early genes Arc, c-fos, and zif268. *J Neurosci.* 21:5089-5098.
42. Hamann S, Monarch ES, Goldstein FC (2002) Impaired fear conditioning in Alzheimer's disease. *Neuropsychologia.* 40:1187-95.
43. Handler M, Yang X, Shen J (2000) Presenilin-1 regulates neuronal differentiation

- during neurogenesis. *Development*. 127:2593-606.
44. Haass C (2004) Take five--BACE and the gamma-secretase quartet conduct Alzheimer's amyloid beta-peptide generation. *EMBO J*. 23:483-8.
45. Haass C, Kaether C, Thinakaran G, Sisodia S (2012) Trafficking and proteolytic processing of APP. *Cold Spring Harb Perspect Med*. 2:a006270.
46. Handler M, Yang X, Shen J (2000) Presenilin-1 regulates neuronal differentiation during neurogenesis. *Development*. 127:2593-606.
47. Hardy J, Selkoe DJ (2002) The amyloid hypothesis of Alzheimer's disease: progress and problems on the road to therapeutics. *Science*. 297:353-356.
48. Hardy J (2006) Has the amyloid cascade hypothesis for Alzheimer's disease been proved? *Curr Alzheimer Res*. 3: 71-73.
49. Hawk JD, Abel T (2011) The role of NR4A transcription factors in memory formation. *Brain Res Bull*. 85: 21-29.
50. Hirano Y, Masuda T, Naganos S, Matsuno M, Ueno K, Miyashita T, Horiuchi J, Saitoe M (2013) Fasting launches CRTC to facilitate long-term memory formation in *Drosophila*. *Science*. 339:443-6.
51. Ho A. and Shen J (2011) Presenilins in synaptic function and disease. *Trends Mol Med*. 17:617-24.
52. Hofer M, Allison SC, Schauer GF, Neuhaus JM, Hall J, Dang JN, Weiner MW, Miller BL, Rosen HJ (2008) Fear conditioning in frontotemporal lobar degeneration and Alzheimer's disease. *Brain*. 131:1646-57.
53. Huff NC, Frank M, Wright-Hardesty K, Sprunger D, Matus-Amat P, Higgins E, Rudy JW (2006). Amygdala regulation of immediate-early gene expression in the hippocampus induced by contextual fear conditioning. *J Neurosci*. 26:1616-1623.
54. Hutton M, Hardy J (1997) The presenilins and Alzheimer's disease. *Hum Mol Genet*. 6:1639-46.
55. Irvine EE, Vernon J, Giese KP (2005) AlphaCaMKII autophosphorylation contributes to rapid learning but is not necessary for memory. *Nat Neurosci*. 8:411-2.
56. Jack CR, Jr., Knopman DS, Jagust WJ, Shaw LM, Aisen PS, Weiner MW, Petersen RC, Trojanowski JQ (2010) Hypothetical model of dynamic biomarkers of the

- Alzheimer's pathological cascade. *Lancet Neurol* 9:119-128.
57. Jagannath A, Butler R, Godinho SI, Couch Y, Brown LA, Vasudevan SR, Flanagan KC, Anthony D, Churchill GC, Wood MJ, Steiner G, Ebeling M, Hossbach M, Wettstein JG, Duffield GE, Gatti S, Hankins MW, Foster RG, Peirson SN (2013) The CRTC1-SIK1 pathway regulates entrainment of the circadian clock. *Cell*. 154:1100-11.
58. Kandel E.R. (2001) The molecular biology of memory storage: a dialog between genes and synapse. *Biosci rep.* Oct;21(5):565-611
59. Kawashima T, Okuno H, Nonaka M, Adachi-Morishima A, Kyo N, Okamura M, Takemoto-Kimura S, Worley PF, Bito H (2009) Synaptic activity-responsive element in the Arc/Arg3.1 promoter essential for synapse-to-nucleus signaling in activated neurons. *Proceedings of the National Academy of Science* 106:316.
60. Khlistunova I, Biernat J, Wang Y, Pichhardt M, von Bergen M, Gazova Z, Mandelkow E, Mandelkow EM (2006) Inducible expression of Tau repeat domain in cell models of tauopathy: aggregation is toxic to cells but can be reversed by inhibitor drugs. *J Biol Chem.* 281:1205-14.
61. Kida, S., Josselyn, S.A., Pena de Ortiz, S., Kogan, J.H., Chevere, I., Masushige, S., and Silva, A.J. (2002). CREB required for the stability of new and reactivated fear memories. *Nat. Neurosci.* 5, 348 – 355.
62. Kim, W.Y. and Shen, J. (2008) Presenilins are required for maintenance of neural stem cells in the developing brain. *Mol. Neurodegener.* 3, 2
63. Kjelstrup KG, Tuvnes FA, Steffenach HA, Murison R, Moser EI, Moser MB (2002) Reduced fear expression after lesions of the ventral hippocampus. *Proc Natl Acad Sci U S A.* 99:10825-30.
64. Klein RL, Dayton RD, Tatom JB, Henderson KM, Henning PP (2008) AAV8, 9, Rh10, Rh43 vector gene transfer in the rat brain: effects of serotype, promoter and purification method. *Mol Ther* 16:89-96.
65. Kornhauser, J.M., Cowan, C.W., Shaywitz, A.J., Dolmetsch, R.E., Griffith, E.C., Hu, L.S., Haddad, C., Xia, Z., and Greenberg, M.E. (2002). CREB transcriptional activity in neurons is regulated by multiple, calcium-specific phosphorylation events. *Neuron* 34, 221 – 233.

66. Kovács KA, Seulet P, Steinmann M, D'Orsi KQ, Magistretti PJ, Alfonso O, Cardinaux JR (2007) TORC1 is a calcium- and cAMP-sensitive coincidence detector involved in hippocampal long-term synaptic plasticity. *Proc Natl Acad Sci U S A* 104:4700–4705.
67. Laudon, H. et al. (2005) A nine-transmembrane domain topology for presenilin 1. *J. Biol. Chem.* 280, 35352–35360
68. Law SW, Conneely OM, DeMayo FJ, O'Malley BW (1992) Identification of a new brain-specific transcription factor, NURR1. *Mol Endocrinol.* 6:2129–2135.
69. Lee, J.H. et al. (2010) Lysosomal proteolysis and autophagy require presenilin 1 and are disrupted by Alzheimer-related PS1 mutations. *Cell* 141, 1146–1158
70. Lee VMY, Goedert M, Trojanowski JQ (2001) Neurodegenerative tauopathies. *Annual Review of Neuroscience.* 24:1121–1159.
71. Li S, Zhang C, Takemori H, Zhou Y, Xiong ZQ (2009) TORC1 regulates activity-dependent CREB-target gene transcription and dendritic growth of developing cortical neurons. *J Neurosci.* 29:2334-43.
72. Lleó A, Saura CA (2011) γ -secretase substrates and their implications for drug development in Alzheimer's disease. *Curr Top Med Chem.* 11:1513-27.
73. Lonze BE and Ginty DD (2002) Function and regulation of CREB family transcription factors in the nervous system. *Neuron* 35, 605 – 623.
74. Lue LF, Kuo YM, Roher AE, Brachova L, Shen Y, Sue L, Beach T, Kurth JH, Rydel RE, Rogers J (1999) Soluble amyloid beta peptide concentration as a predictor of synaptic change in Alzheimer's disease. *Am J Pathol.* 155: 853-62.
75. Lyford GL, Yamagata K, Kaufmann WE, Barnes CA, Sanders LK, Copeland NG, Gilbert DJ, Jenkins NA, Lanahan AA, Worley PF (1995) Arc, a growth factors and activity-regulated gene, encodes a novel cytoskeleton-associated protein that is enriched in neuronal dendrites. *Neuron* 14:433
76. Malkani S, Rosen JB (2000) Induction of NGFI-B mRNA following contextual fear conditioning and its blockade by diazepam. *Brain Res Mol Brain Res.* 80:153-65.
77. Mamiya, N., Fukushima, H., Suzuki, A., Matsuyama, Z., Homma, S., Frankland, P.W., and Kida, S. (2009). Brain region-specific gene expression activation

- required for reconsolidation and extinction of contextual fear memory. *J. Neurosci.* 29, 402 – 413.
78. Maren S (2008) Pavlovian fear conditioning as a behavioral assay for hippocampus and amygdala function: cautions and caveats. *Eur J Neurosci.* 28:1661-6.
79. Maren S, Phan KL, Liberzon I (2013) The contextual brain: implications for fear conditioning, extinction and psychopathology. *Nat Rev Neurosci.* 14:417-28.
80. Mayr B, Montminy M (2001) Transcriptional regulation by the phosphorylation-dependent factor CREB. *Nat Rev Mol Cell Biol.* 2:599-609.
81. Milbrandt J (1988) Nerve growth factor induces a gene homologous to the glucocorticoid receptor gene. *Neuron.* 1:183–188.
82. Milde-Langosch K (2005). The Fos family of transcription factors and their role in tumorigenesis. *Eur. J. Cancer* 41 (16): 2449–61.
83. Moehlmann T , Winkler E , Xia X , Edbauer D , Murrell J , Capell A , Kaether C, Zheng H , Ghetti B , Haass C , Steiner H (2002) Presenilin-1 mutations of leucine 166 equally affect the generation of the Notch and APP intracellular domains independent of their effect on Abeta 42 production. *Proc Natl Acad Sci U S A.* 99:8025-30.
84. Monti B , Bertheletti C , Contestabile A (2006). Subchronic rolipram delivery activates hippocampal CREB and Arc, enhances retention and slows down extinction of conditioned fear. *Neuropsychopharm.* 31:278-286
85. Montminy M R, Sevarino K A, Wagner J A, Mandel G and Goodman R H (1986) Identification of a cyclic-AMP responsive element within the rat somatostatin gene. *Proc. Natl Acad. Sci. USA.* 83, 6682–6686
86. Moser MB, Moser EI (1998) Distributed encoding and retrieval of spatial memory in the hippocampus. *J Neurosci.* 18:7535-42.
87. Neves G I, Cooke S F, Bliss T V (2008) Synaptic plasticity, memory and the hippocampus: a neural network approach to causality. *Nat Rev Neurosci.* 9:65-75.
88. Oddo S, Vasilevko V, Caccamo A, Kitazawa M, Cribbs DH, LaFerla FM (2006) Reduction of soluble A beta and tau, but not soluble A beta alone, ameliorates cognitive decline in transgenic mice with plaques and tangles. *J Biol Chem;*

- 281:39413-23.
89. Ohkura N, Hijikuro M, Yamamoto A, Miki K (1994) Molecular cloning of a novel thyroid/steroid receptor superfamily gene from cultured rat neuronal cells. *Biochem Biophys Res Commun.* 205:1959–1965.
90. Palop JJ, Jones B, Kenyon L, Chin J, Yu GQ, Raber J, Masliah E, Mucke L (2003) Neuronal depletion of calcium-dependent proteins in the dentate gyrus is tightly linked to Alzheimer's disease-related cognitive deficits. *Proc Natl Acad Sci U S A.* 100:9572-7.
91. Parra-Damas A, Valero J, Meng C, España J, Martin E, Ferrer I, Rodriguez-Alvarez J, Saura CA (2014) Crtc1 activates a transcriptional program deregulated at early Alzheimer's disease-related stages *J Neurosci* 34:5776-5787.
92. Phillips R G, LeDoux J E (1992) Differential contribution of amygdala and hippocampus to cued and contextual fear conditioning. *Behav Neurosci.* 106:274-85.
93. Phillips H S, Hains J M, Armanini M, Laramée GR, Johnson SA, Winslow J W (1991) BDNF mRNA is decreased in the hippocampus of individuals with Alzheimer's disease. *Neuron.* 7:695-702.
94. Plath N, Ohana O, Dammermann B, Errington ML, Schmitz D, Gross C, Mao X, Engelsberg A, Ahlke C, Welzl H (2006) Arc/Arg3.1 is essential for the consolidation of synaptic plasticity and memories. *Neuron* 52:437-444.
95. Rogava E, Meng Y, Lee JH, Gu Y, Kawarai T, Zou F, Katayama T, Baldwin CT, Cheng R, Hasegawa H, Chen F, Shibata N, Lunetta KL, Pardossi-Piquard R, Böhm C, Wakutani Y, Cupples LA, Cuenco KT, Green RC, Pinassi L, Rainero I, Sorbi S, Bruni A, Duara R, Friedland RP, Inzelberg R, Hampe W, Bujo H, Song YQ, Andersen OM, Willnow TE, Graff-Radford N, Petersen RC, Dickson D, Der SD, Fraser PE, Schmitt-Ulms G, Younkin S, Mayeux R, Farrer LA, St George-Hyslop P (2007) The neuronal sortilin-related receptor SORL1 is genetically associated with Alzheimer disease. *Nat Genet.* 39:168-77.
96. Rojas P, Joodmardi E, Hong Y, Perlmann T, Ogren SO (2007) Adult mice with reduced Nurr1 expression: a animal model for schizophrenia. *Mol Psychiatry.* 12:756-66.

97. Rosen JB (2004) The neurobiology of conditioned and unconditioned fear: a neurobehavioral system analysis of the amygdala. *Behav Cogn Neurosci Rev* 3:23-41.
98. Ruijter JM, Ramakers C, Hoogaars WM, Karlen Y, Bakker O, van den Hoff MJ, Moorman AF (2009) Amplification efficiency: linking baseline and bias in the analysis of quantitative PCR data. *Nucleic Acids Res.* 37:e45.
99. Sakamoto K, Norona FE, Alzate-Correa D, Scarberry D, Hoyt KR, O'brieta K (2013) Clock and light regulation of the CREB coactivator CRTC1 in the suprachiasmatic circadian clock. *J Neurosci.* 33:9021-7.
100. Santacruz K, Lewis J, Spires T, Paulson J, Kotilinek L, Ingelsson M, Guimaraes A, DeTure M, Ramsden M, McGowan E, Forster C, Yue M, Orne J, Janus C, Mariash A, Kuskowski M, Hyman B, Hutton M, Ashe KH (2005) Tau suppression in a neurodegenerative mouse model improves memory function. *Science.* 309:476-81.
101. Satoh J, Tabunoki H, Arima K (2009) Molecular network analysis suggests aberrant CREB-mediated gene regulation in the Alzheimer disease hippocampus. *Dis Markers.* 27:239-52.
102. Saura CA, Choi SY, Beglopoulos V, Malkani S, Zhang D, Shankaranarayana Rao BS, Chattarji S, Kelleher RJ 3rd, Kandel ER, Duff K, Kirkwood A, Shen J (2004) Loss of presenilin function causes impairments of memory and synaptic plasticity followed by age-dependent neurodegeneration. *Neuron* 42, 23–36
103. Saura CA, Valero J (2011) The role of CREB signaling in Alzheimer's disease and other cognitive disorders. *Rev Neurosci.* 22:153-69.
104. Scheff SW, Price DA (2003) Synaptic pathology in Alzheimer's disease: a review of ultrastructural studies. *Neurobiol Aging.* 24:1029-46.
105. Scream RA, Conkright MD, Katoh Y, Best JL, Canettieri G, Jeffries S, Guzman E, Niessen S, Yates JR 3rd, Takemori H, Okamoto M, Montminy M (2004) The CREB coactivator TORC2 functions as a calcium- and cAMP sensitive coincidence detector. *Cell* 119:61–74.
106. Sekeres MJ, Mercaldo V, Richards B, Sargin D, Mahadevan V, Woodin MA, Frankland PW, Josselyn SA (2012) Increasing CRTC1 function in the dentate

- gyrus during memory formation or reactivation increases memory strength without compromising memory quality. *J Neurosci.* 32:17857-68.
107. Shen J, Bronson RT, Chen DF, Xia W, Selkoe DJ, Tonegawa S (1997) Skeletal and CNS defects in Presenilin-1-deficient mice. *Cell.* 89:629-39.
108. Shen J, Kelleher RJ 3rd (2007) The presenilin hypothesis of Alzheimer's disease: evidence for a loss-of-function pathogenic mechanism. *Proc Natl Acad Sci U S A.* 104:403-9.
109. Sheng M, Thompson M A, Greenberg M E (1991) CREB: a Ca (2+)-regulated transcription factor phosphorylated by calmodulin-dependent kinases. *Science.* 252:1427-30.
110. Sindreu CB, Scheiner ZS, Storm DR (2007) Ca²⁺-stimulated adenylyl cyclases regulate ERK-dependent activation of MSK1 during fear conditioning. *Neuron.* 53:79-89.
111. Snyder EM, Nong Y, Almeida CG, Paul S, Moran T, Choi EY, Nairn AC, Salter MW, Lombroso P J, Gouras G K, Greengard P (2005) Regulation of NMDA receptor trafficking by amyloid-beta. *Nat Neurosci.* 8:1051-8.
112. Small BJ, Fratiglioni L, Viitanen M, Winblad B, Bäckman L (2000) The course of cognitive impairment in preclinical Alzheimer disease: three- and 6-year follow-up of a population-based sample. *Arch Neurol.* 57:839-44.
113. Song I, Huganir R L (2002) Regulation of AMPA receptors during synaptic plasticity. *Trends in neurosciences* 25:578-588.
114. Sperling R, Chua E, Cocchiarella A, Rand-Giovannetti E, Poldrack R, Schacter DL, Albert M (2003) Putting names to faces: successful encoding of associative memories activates the anterior hippocampal formation. *Neuroimage.* 20:1400-10.
115. Smith DL, Pozueta J, Gong B, Arancio O, Shelanski M (2009) Reversal of long-term dendritic spine alterations in Alzheimer disease models. *Proc Natl Acad Sci U S A.* 106:16877-82.
116. Song I, Huganir RL (2002) Regulation of AMPA receptors during synaptic plasticity. *Trends Neurosci.* 25:578-88.
117. Squire LR, Zola-Morgan S (1991) The medial temporal lobe memory system. *Science.* 253:1380-6.

118. Steiner H, Duff K, Capell A, Romig H, Grim MG, Lincoln S, Hardy J, Yu X, Picciano M, Fichtler K, Citron M, Kopan R, Pesold B, Kreck S, Baader M, Tomita T, Iwatsubo T, Baumeister R, Haass C (1999) A loss of function mutation of presenilin-2 interferes with a myloid beta-peptide production and notch signaling. *J Biol Chem.* 274:28669-73.
119. Steward O, Wallace CS, Lyford GL, Worley PF (1998) Synaptic activation causes the mRNA for the leg Arc to localize selectively near activated postsynaptic sites on dendrites. *NEURON-CAMBRIDGE-MA.* 21:741-751.
120. Steward O, Worley PF (2001). Selective targeting of newly synthesized Arc mRNA to active synapses requires NMDA receptor activation. *Neuron.* 30:227-240.
121. Thal DR, Rüb U, Orantes M, Braak H (2002) Phases of A beta-deposition in the human brain and its relevance for the development of AD. *Neurology.* 58:1791-800.
122. Than TA, Lou H, Ji C, Win S, Kaplowitz N (2011) Role of cAMP-responsive element-binding protein (CREB)-regulated transcription coactivator 3 (CRTC3) in the initiation of mitochondrial biogenesis and stress response in liver cells. *J Biol Chem.* 286:22047-54.
123. Thinakaran G, Borchelt DR, Lee MK, Slunt HH, Spitzer L, Kim G, Ratovitsky T, Davenport F, Nordstedt C, Seeger M, Hardy J, Levey AI, Gandy SE, Jenkins NA, Copeland NG, Price DL, Sisodia SS (1996) Endoproteolysis of presenilin 1 and accumulation of processed derivatives in vivo. *Neuron,* 17:181–190.
124. Tischmeyer W, Grimm R (1999) Activation of immediate early genes and memory formation. *Cellular and Molecular Life Sciences* 55:564-574.
125. Tong L, Thornton PL, Balazs R, Cotman CW (2001) Beta -amyloid-(1-42) impairs activity-dependent cAMP-response element-binding protein signaling in neurons at concentrations in which cell survival is not compromised. *J Biol Chem.* 276:17301-6.
126. Treves A, Rolls ET (1994) Computational analysis of the role of the hippocampus in memory. *Hippocampus.* 4:374-91.
127. Tronson NC, Wiseman SL, Neve RL, Nestler EJ, Olausson P, Taylor JR (2012)

- Distinctive roles for amygdalar CREB in reconsolidation and extinction of fear memory. *Learn Mem.* 19:178-81.
128. Tu, H. et al. (2006) Presenilins form ER Ca²⁺ leak channels, a function disrupted by familial Alzheimer's disease-linked mutations. *Cell* 126, 981–993
129. Tully T, Bourchouladze R, Scott R, Tallman J (2003) Targeting the CREB pathway for memory enhancers. *Nat Rev Drug Discov.* 2:267-77.
130. Tulving E, Kapur S, Craik F I, Moscovitch M, Houle S (1994) Hemispheric encoding/retrieval asymmetry in episodic memory: positron emission tomography findings. *Proc Natl Acad Sci U S A.* 91:2016-20.
131. van der Meulen M, Lederrey C, Rieger S W, van Assche M, Schwartz S, Vuilleumier P, Assal F (2012) Associative and semantic memory deficits in amnesic mild cognitive impairment as revealed by functional magnetic resonance imaging. *Cogn Behav Neurol.* 25:195-215.
132. Villiger JW, Dunn AJ (1981) Phosphodiesterase inhibitors facilitate memory for passive avoidance conditioning. *Behav Neural Biol.* 31:354-9.
133. Vitolo O V, Sant'Angelo A, Costanzo V, Battaglia F, Rancio O, Shelanski M (2002) Amyloid beta -peptide inhibition of the PKA/CREB pathway and long-term potentiation: reversibility by drugs that enhance cAMP signaling. *Proc Natl Acad Sci U S A.* 99:13217-21.
134. von Herten LS, Giese KP (2005) Memory reconsolidation engages only a subset of immediate-early genes induced during consolidation. *J Neurosci.* 25:1935-42.
135. Walter J, Capell A, Grunberg J, Pesold B, Schindzielorz A, Prior R, Podlisny MB, Fraser P, Hyslop P S, Selkoe D J, Haass C (1996) The Alzheimer's disease-associated presenilins are differentially phosphorylated proteins located predominantly within the endoplasmic reticulum. *Mol Med.* 2:673–691.
136. Wang Y, Inoue H, Ravnskjaer K, Viste K, Miller N, Liu Y, Hedrick S, Vera L, Montminy M (2010) Targeted disruption of the CREB coactivator Crtc2 increases insulin sensitivity. *Proc Natl Acad Sci U S A.* 107:3087-92.
137. Watts AG, Sanchez-Watts G, Liu Y, Aguilera G (2011) The distribution of messenger RNAs encoding the three isoforms of the transducer of regulated cAMP responsive element binding protein activity in the rat forebrain. *J Neuroendocrinol.*

- 23:754-66.
138. WHO. Dementia a public health priority. 2012
139. Wines-Samuelson M, Shen J (2005) Presenilins in the developing, adult, and aging cerebral cortex. *Neuroscientist*. 11:441-51.
140. Won J, Silva AJ (2008) Molecular and cellular mechanisms of memory allocation in neuronetworks. *Neurobiol Learn Mem*. 89:285-92.
141. Wu, G.Y., Deisseroth, K., and Tsien, R.W. (2001). Activity-dependent CREB phosphorylation: convergence of a fast, sensitive calmodulin kinase pathway and a slow, less sensitive mitogen-activated protein kinase pathway. *Proc. Natl. Acad. Sci. USA* 98, 2808 – 2813.
142. Xiao Q, Castillo SO, Nikodem VM (1996) Distribution of messenger RNAs for the orphan nuclear receptors Nurr1 and Nur77 (NGFI-B) in adult rat brain using in situ hybridization. *Neuroscience*. 75:221-30.
143. Yamamoto-Sasaki M, Ozawa H, Saito T, Rösler M, Riederer P (1999) Impaired phosphorylation of cyclic AMP response element binding protein in the hippocampus of dementia of the Alzheimer type. *Brain Res*. 824:300-3.
144. Yin, J.C., Del Vecchio, M., Zhou, H., and Tully, T. (1995). CREB as a memory modulator: induced expression of a dCREB2 activator isoform enhances long-term memory in *Drosophila*. *Cell* 81,107 – 115.
145. Yin, J.C., Wallach, J.S., Del Vecchio, M., Wilder, E.L., Zhou, H., Quinn, W.G., and Tully, T. (1994). Induction of a dominant negative CREB transgene specifically blocks long-term memory in *Drosophila*. *Cell* 79, 49 – 58.
146. Yu H, Saura CA, Choi SY, Sun LD, Yang X, Handler M, Kawarabayashi T, Younkin L, Fedels B, Wilson MA, Younkin S, Kandel ER, Kirkwood A, Shen J (2001). APP processing and synaptic plasticity in presenilin-1 conditional knockout mice. *Neuron* 31, 713-726.
147. Zhang C, Wu B, Beglopoulos V, Wines-Samuelson M, Zhang D, Dragatsis I, Südhof TC, Shen J (2009) Presenilins are essential for regulating neurotransmitter release. *Nature*. 460:632-6.
148. Zhang X, Odom DT, Koo SH, Conkright MD, Canettieri G, Best J, Chen H, Jenner R, Herbolsheimer E, Jacobsen E, Adam S, Ecker JR, Emerson B,

-
- Hogenesch JB, Unterman T, Young RA, Montminy M. (2005) Genome-wide analysis of cAMP-response element binding protein occupancy, phosphorylation, and target gene activation in human tissues. *Proc Natl Acad Sci U S A.* 102:4459-64.
149. Zhou Y, Wu H, Li S, Chen Q, Cheng XW, Zheng J, Takemori H, Xiong ZQ. (2006) Requirement of TORC1 for late-phase long-term potentiation in the hippocampus. *PLoS One.* 1:e16.
150. Zola-Morgan S, Squire LR, Rempel NL, Clower RP, Amaral DG (1992) Enduring memory impairment in monkeys after ischemic damage to the hippocampus. *J Neurosci.* 12:2582-96.